



**GROUNDWATER ASSESSMENT IN RELATION TO
CLIMATIC VARIATION: CASE STUDY OF THE
LICHTENBURG KARST AQUIFER**

Lindelani Lalumbe

Student number: 1258499

In partial fulfilment for the Master of Science in Hydrogeology

Supervisor: Prof Tamiru Abiye

School of Geosciences

University of the Witwatersrand, Johannesburg

July 2018

Declaration

I **LINDELANI LALUMBE** declare that the master's degree research report that I herewith submit is my own and ideas from other sources have been dually acknowledged. This work is submitted in partial fulfilment of the Master of Science degree in Hydrogeology at the University of the Witwatersrand, Johannesburg, South Africa. This work has never been submitted before in any university for any examination or degree according to my knowledge.

Name: Lindelani Lalumbe

Signature

Date

Place



July 2018

Johannesburg

Acknowledgements

Firstly I would like to thank God for giving me an opportunity to study further.

I would also like to thank my family for the support throughout my studies and always encouraging me when I was giving up. Special thanks to my Uncle “Naledzani Amos Lalumbe” and my Aunt “Mavhungu Emily Lalumbe”.

Special thanks to Miss Dineo Mamatho for the continuous support and encouragement throughout my studies and always believing in me.

I would like to thank the Department of Water and Sanitation (DWS) for giving me permission to use their database and an opportunity to study further. Special thanks to the HYDSTRA, CHART and WMS team for the assistance during my studies.

I would like to thank the South African Weather Services (SAWS) for providing me with climate data for this study.

Special thanks to Prof. Tamiru Abiye for the support, guidance and constructive criticism during the research and the entire course.

Dedication

This study is dedicated to my late family members who supported my dreams as a child:

1. My Mother Mmbulungeni Josephine Lalumbe
2. My Grandmother Nditsheni Anna Lalumbe
3. My Grandfather Mubvafhi Besenia Lalumbe
4. My Uncle Meshack Thinamaano Lalumbe

Abstract

Monitoring and assessment of groundwater resources in the karst belt in South Africa has been conducted by the Department of Water and Sanitation (DWS) for several years as a special monitoring program as it was considered as a vulnerable aquifer. This was done to determine the groundwater potential for bulk water supply and also the impact of climatic variation and over abstraction on the availability of groundwater in the area.

The impact of climatic variation on the Lichtenburg dolomitic aquifer was assessed based on the declining water table from 2013 to 2017. The study analysed previous studies conducted in relation to past drought events in Southern Africa. The study established that climatic variation alone did not result in the decline of groundwater table. Over abstraction was also contributed to the decline of the water table owing to high demand in water use. The standardized precipitation index (SPI) calculated in 2015 corresponds with the declining groundwater table.

The groundwater quality of the aquifer was not impacted by climatic variation. The 20 years groundwater quality data indicated that there was no major difference in water quality over different climatic conditions beside slightly elevated sodium in the September 2016 results. The main water facies was represented by Ca-Mg-HCO₃ type water. The stable isotope results indicated the possibility of mixing with deep circulating karstic springs and also that evaporation took place before infiltration in some part of this aquifer. The conceptual model indicates quantitative values and findings determined by the study.

Keywords: *Abstraction, Aridity, Climatic variation, Dolomite, Drought, Groundwater, Isotopes, Karst aquifer, Recharge.*

Table of Contents

Declaration.....	i
Acknowledgements.....	ii
Dedication.....	iii
Abstract.....	iv
List of figures.....	vii
List of tables.....	viii
List of abbreviations.....	ix
Chapter 1: Introduction.....	1
1.1. Background.....	1
1.2. Problem statement.....	2
1.3. Research aim and objectives.....	3
Chapter 2: Site Description.....	3
2.1. Location.....	3
2.2. Physiography.....	4
2.3. Climate.....	6
2.4. Geology.....	7
2.4.1. Regional geology.....	7
2.4.2. Local geology.....	10
2.5. Hydrogeological settings.....	13
Chapter 3: Literature review.....	21
3.1. Introduction.....	21
3.2. El Nino- Southern Oscillation (ENSO).....	21
3.2.1. El Nino in Southern Africa.....	22
3.3. Aridity conditions in Southern Africa.....	23
3.4. The impact of climatic variation on groundwater resources.....	26
3.5. Concepts of groundwater assessment.....	28

3.5.1. Storativity and transmissivity.....	28
3.5.2. Groundwater recharge.....	29
3.5.2.1. Chloride Mass Balance (CMB).....	30
3.5.3. Groundwater quality	31
3.5.4. Environmental isotopes.....	32
3.6. Previous studies conducted in semi-arid regions and in karst environments	32
3.6.1. International studies	32
3.6.2. Local studies	33
Chapter 4: Methodology	35
4.1. Desktop study.....	35
4.2. Fieldwork	35
4.2.1. Groundwater level measurements.....	35
4.2.2. Sampling and analysis.....	36
4.2.2.1. Major ion chemistry	36
4.2.2.2. Environmental stable isotopes of ^{18}O and ^2H	38
Chapter 5: Results and discussions	38
5.1. Recharge estimation using Chloride Mass Balance	38
5.2. Analysis of groundwater level trends against rainfall.....	39
5.3. Field parameters analysis	48
5.4. Laboratory parameters analysis	50
5.4.1. Major ion.....	50
Chapter 6: Conclusion	59
Chapter 7: References	60

List of figures

Figure 1: Study area location map	4
Figure 2: Topographic contour map of the study area	5
Figure 3: Mean annual precipitation of Lichtenburg karst aquifer (rainfall station situated in the town of Lichtenburg) with the arrow indicating the possible 2015 El Nino event (Data source: SAWS).....	6
Figure 4: Historical temperature and Mean Annual Precipitation for Lichtenburg karst aquifer (Data source: SAWS), with arrows indicating past El Nino event as well as the 2015 El Nino event.....	7
Figure 5: Stratigraphy of the North West dolomitic sequence (Eriksson et al., 2006)	10
Figure 6: Geology of the study area with boreholes of interest (Modified for C31A quaternary catchment from Eriksson et al., 2006).....	12
Figure 7: Groundwater flow direction	16
Figure 8: Aquifer map of the study area (Modified for C31A quaternary catchment from Barnard, 2000), with arrows showing cross sections lines.	17
Figure 9: Hydrogeological Cross-section A-B (Modified from Barnard, 2000), with arrow indicating groundwater flow direction (hydraulic gradient: 0.0010 and vertical exaggeration factor of 10)	18
Figure 10: Hydrogeological Cross-section C-D (Modified from the Barnard, 2000), with arrow indicating groundwater flow direction (hydraulic gradient: 0.0010 and vertical exaggeration factor of 10)	19
Figure 11: Local scale borehole yield map	20
Figure 12: 1985 to 2017 North West MAP-Temperature data (Source of data: SAWS, 2017), with arrows indicating past El Nino events (Source of data: UNDP, 2017).....	22
Figure 13: Aridity conditions in Southern Africa (Adopted from Abiye, 2016)	24
Figure 14: March 2015 to February 2016 standardized precipitation index (Adopted from Abiye, 2016)	25
Figure 15: Illustration of the hydrological cycle (Source: Stagl et al., 2014)	27
Figure 16: Picture taken during measurement of groundwater level at C3N0036.....	36
Figure 17: Sampling procedure used for major ion chemistry sampling	37
Figure 18: Field Parameters measurements on site.....	37
Figure 19: Relationship between groundwater levels (C3N0544), rainfall and temperature.....	40
Figure 20: Relationship between groundwater levels (C3N0553), rainfall and temperature.....	41
Figure 21: Relationship between groundwater levels (C3N0036), rainfall and temperature.....	42
Figure 22: Four years period of groundwater level trends at three boreholes.....	44
Figure 23: Groundwater level fluctuations from 1990 until 2017 with arrows indicating past drought events (HYDSTRA: DWS).....	45
Figure 24: Boreholes location in respect to the rainfall station (Modified from DWS, 2006)	47
Figure 25: EC-pH trends over a period of 20 years (Data source: Chart, DWS).....	48
Figure 26: Piper diagram plot for major ions from 1997 to 2016 (ZQMLTG1).....	53
Figure 27: Piper diagram plot for C3N0544 and ZQMLTG1	55
Figure 28: Stable isotope analysis plot on the Pretoria LMWL.....	57
Figure 29: Conceptual hydrogeological model of the study area	58

List of tables

Table 1: Lithology report for ZQMLTG1	14
Table 2: Recharge estimation based on sampled chloride concentration in rainfall (C3N0544).....	39
Table 3: Summary of field measurements at all Groundwater level monitoring stations (Borehole depth: NGA)	39
Table 4: Field details of groundwater quality monitoring station ZQMLTG1 (Source: NGA, DWS)	48
Table 5: Field measurement results for ZQMLTG1 (Source: NGA, DWS)	50
Table 6: Major ion composition (mg/l) for ZQMLTG1 (Source: DWS CHART)	51
Table 7: Ion balance from 2012 to 2016 (DWS CHART)	52
Table 8: Major ion results for C3N0544 (mg/l)	52
Table 9: Stable isotopes results	56

List of abbreviations

a	Annum
ARC	Agricultural Research Council
CGS	Council for Geosciences
CMB	Chloride Mass Balance
CRD	Cumulative Rainfall Departure
°C	Degree Celsius
DWA	Department of Water Affairs
DWAF	Department of Water Affairs and Forestry
DWS	Department of Water and Sanitation
EC	Electrical Conductivity
ENSO	El Nino- Southern Oscillation
GMWL	Global Meteoric Water Line
GNIP	Global Network of Isotopes In Precipitation
GRAI	Groundwater Resource Assessment 1
GRAII	Groundwater Resource Assessment 2
GWR	Groundwater Rule
IAEA	International Atomic Energy Agency
LMWL	Local Meteoric Water Line
Mamsl	Meters above mean sea level
MAP	Mean Annual Precipitation
Mbgl	Meter below ground level

mm/a	Millimetre per annum
mm/m	Millimetre per month
NGA	National Groundwater Archive
NGDB	National Groundwater Database
SAWS	South African Weather Service
SPI	Standardized Precipitation Index
TDS	Total Dissolved Solids
TU	Tritium Unit
WARMS	Water Authorization and Registration Management System
WHO	World Health Organization
WMS	Water Management System

Chapter 1: Introduction

1.1. Background

International Research Institute for climate and society (IRI) predicted that there is a big chance for El Nino to develop towards the end of 2014 in South Africa (FEWSNET, 2014). The El Nino event is associated with low rainfall usually during high rainfall seasons in semi-arid Southern Africa (December-March). The El Nino effect resulted in most dams in South Africa having very low water levels. Department of Water and Sanitation (DWS) together with water boards and municipalities adopted water supply restriction in major towns (DWS, 2016).

South Africa is regarded as a water scarce country located in a semi-arid climatic condition with an average precipitation of 500 mm/a compared to the world average rainfall of 860 mm/a (Dennis & Dennis, 2012). Any climatic variations could have severe impacts on water resources in the country. Rainfall in this semi-arid region of South Africa decreases from East to West (Dennis & Dennis, 2012).

The Lichtenburg karst aquifer (693 km²) is located north of the town of Lichtenburg, in the North West Province. The area is part of Malmani dolomite, identified as the Lichtenburg unit. Groundwater in this karst aquifer occurs in the fractures and also in the dissolution cavities. These fractures and cavities formed over the geological times resulting from carbonate dissolution by precipitation (Bredenkamp et al., 1997).

A lot of studies have been done in the Malmani dolomite over the years and mostly on the estimation of recharge (Enslin, 1970; Fleisher, 1981; Foster, 1987; Bredenkamp, 1987; 1997; 2009).

DWS has an ongoing monitoring program in the study area. Monitoring data show a rapid decline in water table in the Lichtenburg karst aquifer. Groundwater abstraction rate is very extensive in the Lichtenburg compartment. The main use of groundwater is for bulk water supply and irrigation as it is the farming area with industries. The aquifer might be vulnerable to pollution due to over-exploitation (DWAF, 2006). The DWS water authorization and registration management system (WARMS) indicated that the groundwater resource in the Lichtenburg dolomitic unit is being over utilized.

There is one water quality monitoring borehole in the study area with reliable historical data. The data will be useful in determining the geochemical evolution of different climatic conditions as this will be helpful in understanding the aquifer better.

In order to understand how the aquifer is behaving in relation to climatic variations we need to understand current abstraction rate, available reserve and also recharge estimation in the Lichtenburg karst aquifer in Figure 1. It will also be useful to understand the reaction of groundwater level to precipitation throughout the hydrological year.

1.2. Problem statement

According to the WARMS system, there are 201 known groundwater users in quaternary catchment C31A and most boreholes are clustered in the Lichtenburg karst aquifer. Most users are tapping groundwater for agricultural purposes (irrigation and livestock), followed by industries, water supply and mining. DWA uses systems such as GRA2, GWR and WARMS for reserve determination. All these system indicate that this area is being over-exploited. Current abstraction rate is at 37.3 million m³/a, and the allocable reserve was determined at 26.4 million m³/a.

A decline in groundwater levels has been observed in the monitored boreholes in the Lichtenburg unit. With a decline in groundwater level in this area, that also includes large part of the Lichtenburg dolomite compartment, a serious re-evaluation of resource management needs to be considered in order to protect the resource. The behaviour of this aquifer in relation to climatic variation needs to be well documented if the aquifer is going to be considered for more bulk water supply in the area.

DWAF (2006) stated that groundwater level decline is one of the primary mechanisms triggering sinkhole formation. South African geological hazards observation system atlas map (2015) from the Council for Geoscience (CGS) also classifies the study area as a vulnerable site to sinkholes and also a very high vulnerable area to pollution. Lack of assessment, management and planning can lead to dolomite resources being detrimentally impacted in future during low rainfall periods.

1.3. Research aim and objectives

The most important aim of the study is to understand the behaviour of the dolomitic aquifer during very low rainfall and high temperature seasons compared to high rainfall seasons. This will be achieved by the following objectives:

- Determine the hydro-geochemical evolution in the aquifer
- Estimating recharge using CMB
- Evaluating monitoring data and comparing it to various climatic conditions over the years.
- Analysis of groundwater level trends.

Chapter 2: Site Description

2.1. Location

The study area is located just north of the town of Lichtenburg in the North West Province (Figure 1). The Lichtenburg compartment is part of the Malmani dolomite sequence that stretches from North West to Gauteng province. The study area is located within the C31A quaternary catchment in the Lower Vaal water management area.

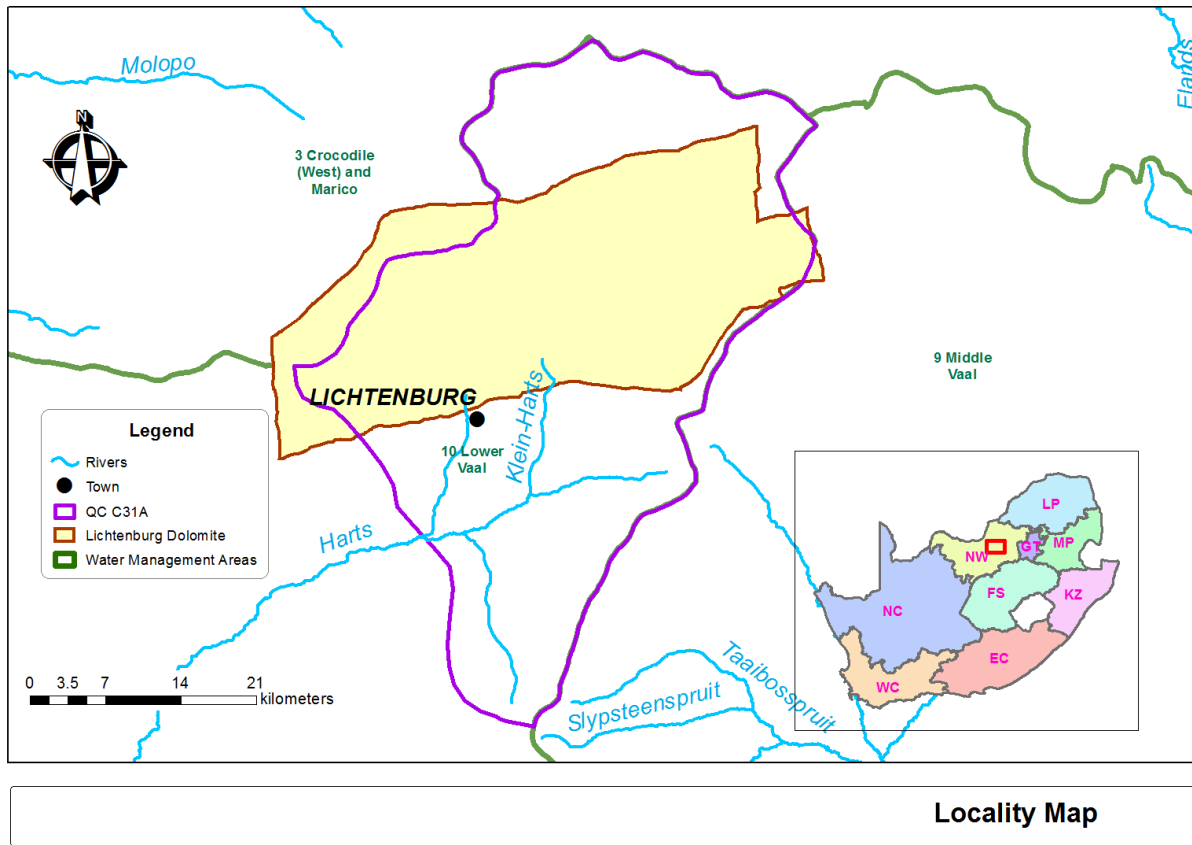


Figure 1: Study area location map

2.2. Physiography

The study area lies between 1480 m and 1540 m above sea level (Figure 2). It is comprised of a large, undulating plain characterised by the absence of any marked topographical features rather than the moderate to low relief plains. Structures such as faults and Blaauwbank dyke control groundwater occurrence in the area (Obbes, 2001).

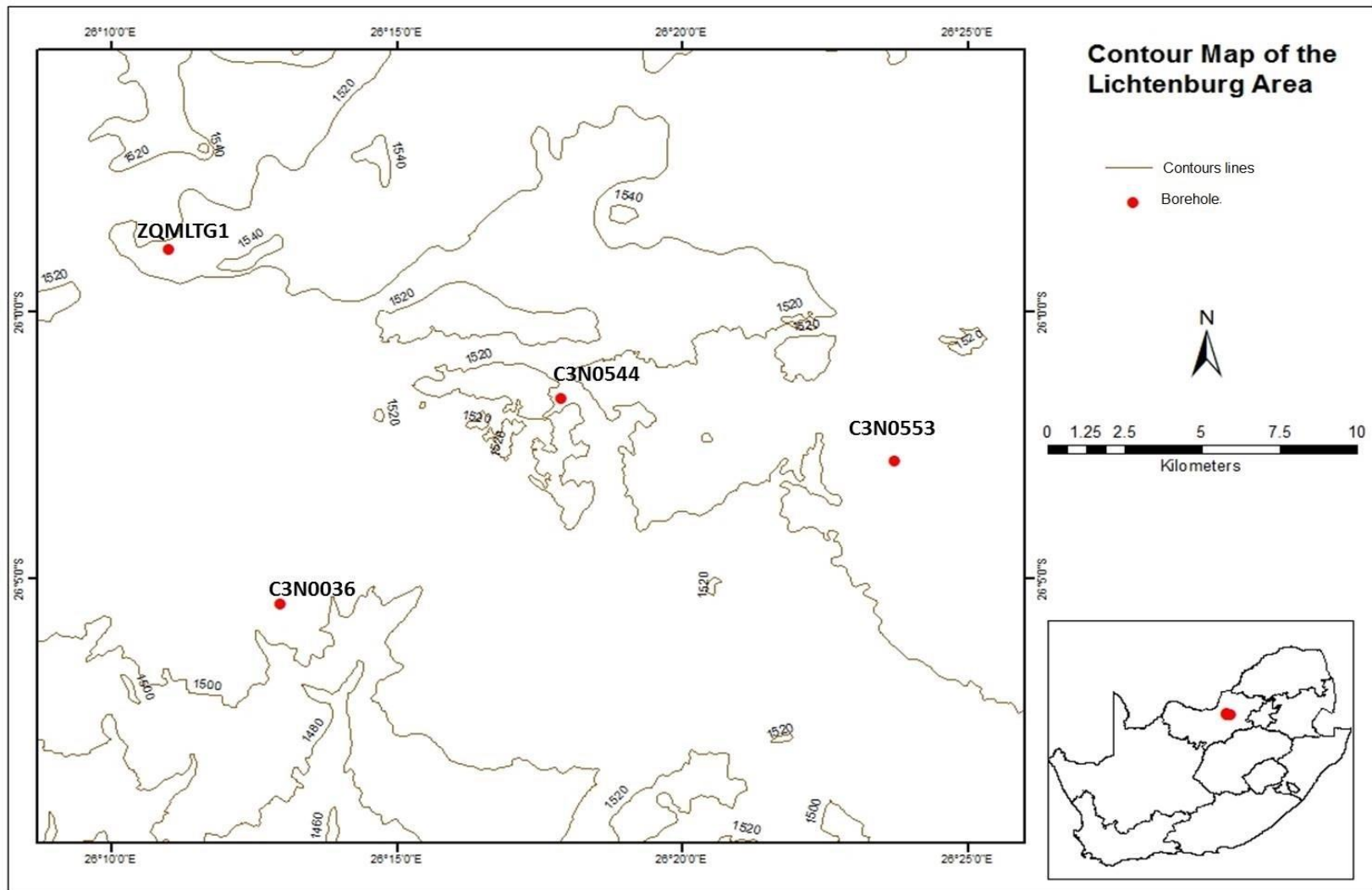


Figure 2: Topographic contour map of the study area

2.3. Climate

Lichtenburg karst aquifer is situated in the semi-arid region of western part of South Africa. This region is characterized by strong seasonal rainfall that mostly occurs as summer thunderstorms. Annual rainfall in Lichtenburg area ranges between 400 to 730 mm based on the four years data. Average rainfall in the four hydrological years is 538.95 mm/a. The lowest total rainfall was recorded in 2015/16 (430.6 mm) and the highest in 2016/17 (720.8 mm). The hydrological year's rainfall data is presented in Figure 3. For this purpose station number 04722780 of SAWS was used. Annual average temperature ranges from 18 to 28°C in this region. Minimum (1°C) and maximum (32°C) temperatures are experienced in July and January, respectively.

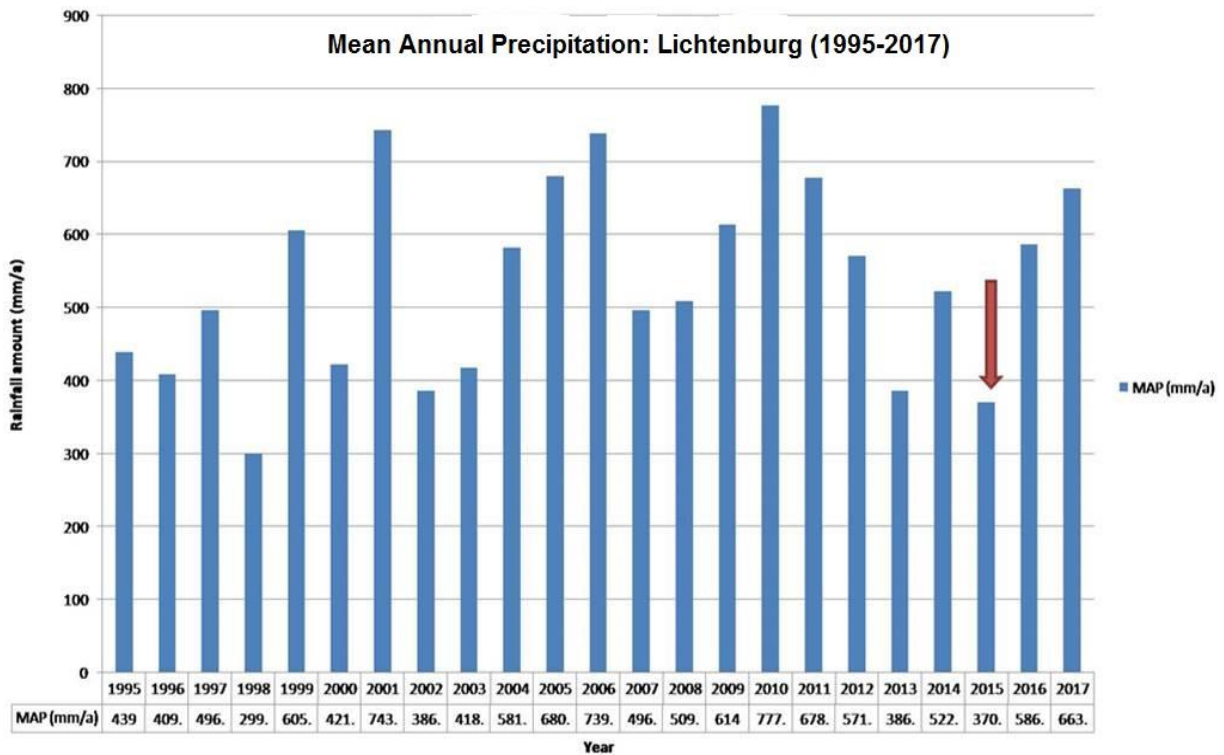


Figure 3: Mean annual precipitation of Lichtenburg karst aquifer (rainfall station situated in the town of Lichtenburg) with the arrow indicating the possible 2015 El Nino event (Data source: SAWS)

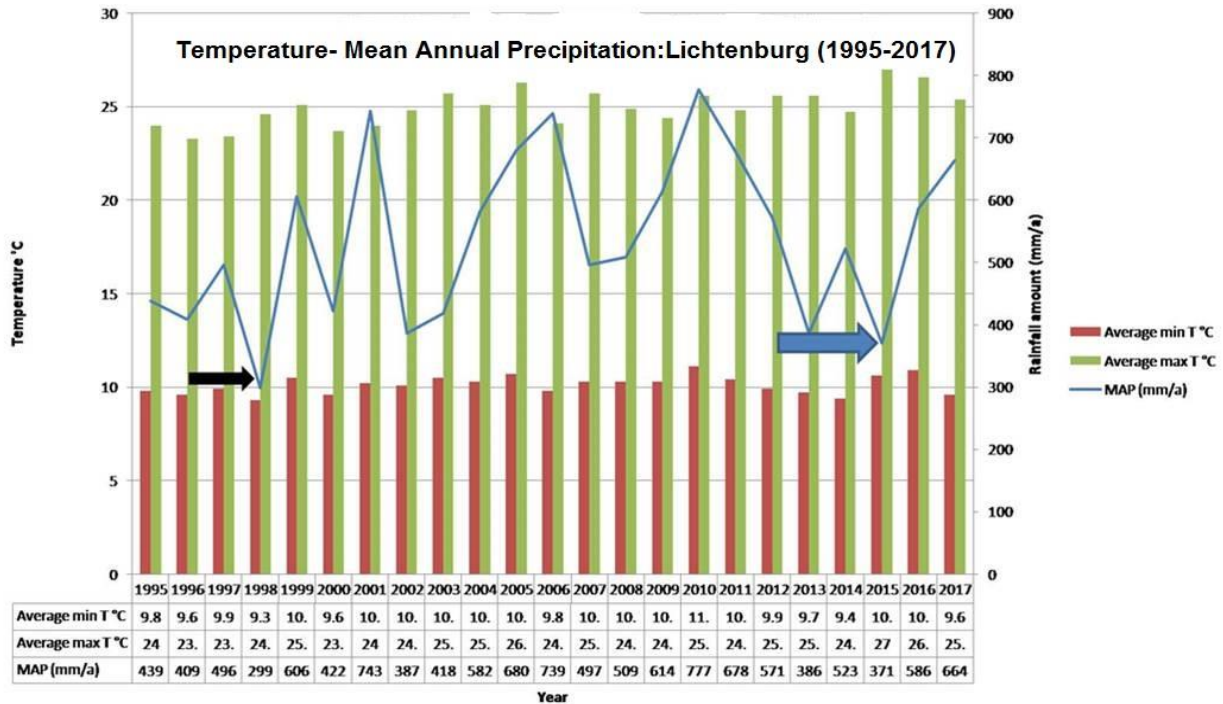


Figure 4: Historical temperature and Mean Annual Precipitation for Lichtenburg karst aquifer (Data source: SAWS), with arrows indicating past El Niño event as well as the 2015 El Niño event.

2.4. Geology

2.4.1. Regional geology

The Lichtenburg dolomitic unit falls within Malmani Subgroup of the Chuniespoort Group, which instead is part of the Transvaal Supergroup (Figure 5). This was formed around 2.7 billion years ago and over the years it has been deformed tectonically, intruded and faulted by dykes and some other structures (Eriksson et al., 2006).

The Transvaal Supergroup covers other three structural basins of the Kaapvaal craton, where iron formation, minor silica clastics and carbonates were deposited (Eriksson et al., 2006). Grikualand west and Transvaal basins are located in South Africa and the other basin is situated in Botswana known as the Kanye basin (Eriksson et al., 2006). Beukes (1987) mentioned that the Transvaal Supergroup constitutes one of the earliest carbonate successions in the world. This carbonate

succession overlies formations from the Archaen basement, Witwatersrand and Ventersdorp Supergroups (Beukes, 1987).

The Malmani Subgroup is underlain by the Black Reef Formation (Clastic sedimentary series of quartzite, shale and conglomerate). The base of the Transvaal Supergroup is constituted by the quartzite of the Black Reef Formation (Button, 1970). Coetzee (1996) defined the Black Reef Formation as the sedimentary succession between the Archean rocks and the lowermost dolomitic bed.

In this Malmani dolomite sequence, various formations exist with varying composition overlying the Black Reef Formation. As presented in Figure 5, dolomite of the Malmani Subgroup comprises five formations, from base to bottom: the Oaktree, Monte Christo, Lyttelton, Eccles and Frisco formations (Eriksson et al., 2006).

The Oaktree Formation (200 m thick) at the base is composed of chert-poor dolomite (dark) with shale (Obbes, 1995). Shale marker beds, large stromatolitic domes, tuffe marker and the convolute chert marker are dominant in this Formation. The contact linking the overlying Monte Christo Formation with Oaktree Formation is gradual and dolomite colour change from dark brown to light grey and chert content increases (Obbes, 1995).

The chert-rich Monte Christo Formation (700 m thick) contains oolitic chert. The Formation has a coarse texture, moderate relief, streaky appearance and well characterized bedding traces. Dolerite dykes of Precambrian intruded this Formation striking from east-west and north-south. Erosion and dissolution that occurred along lineaments that are structurally controlled led to a karst topography related to sinkhole formations (SACS, 1980).

The chert-poor Lyttelton Formation (150 m thick) overlies the Monte Christo Formation and is characterized by chocolate brown dolomite. More chert is contained at the lower part of this succession compared to the central part (Clay, 1981). This Formation is also characterized by megadomal stromatolites and cross-bedded dolarenite beds are common. Relatively subdued topography, dark tone and bedding traces that are poorly defined are common. The Eccles Formation overlies this Formation and the contact is gradational and is where the dolomite colour change from dark brown to grey with increasing chert content (Clay, 1981).

Interbedded light grey dolomite and chert bands are common in Eccles Formation (380 m thick) (Obbes, 1995). This Formation is characterized by outstanding bedding traces from aerial photographs. At the top of the Eccles formation, chert breccia occurs. A dark brown color chert-poor dolomite occurs on top of the chert shale breccias. Silicified chert breccia caps the Eccles Formation with a marker unit (Obbes, 1995).

The uppermost section of the Malmani Subgroup is overlain by the Rooihoogte Formation (conglomerate breccias, shale and quartzite) and some sections are overlain by the sequence of sedimentary rocks of the Timeball Hill Formation of the Pretoria Group. The Malmani Subgroup dips to the north and lies underneath the Pretoria Group as presented in figure 5.

Much younger mudrock and shale of the Vryheid Formation (Karoo Supergroup) covers the eastern side of the Malmani Subgroup. This younger Formation is usually underlain by shale and diamictite of the Dwyka Group. In the north east and west of Lichtenburg a younger unconsolidated alluvial deposits overlie dolomite.

System	Sequence	Group	Formation		Lithology and Member	Thick-ness (m)	
PERM-CARBONIFEROUS	KAROO	ECCA			Sandstone		
					Mudstone Carbonaceous Shale, coal		
					Sandstone		
					Shale		
					Diamictite		
PROTEROZOIC	TRANSVAAL	PRETORIA	TIMEBALL HILL		Shale	270 - 660	
					Diamictite		
					Klapperkop Quartzite Mb wacke and ferruginous quartzite Graphitic and silty shale		
			ROOIHOOGTE		Quartzite	Shale	10 - 150
						Bevets Conglomerate Member Breccia	
			CHUNIESPOORT	ECCLES		Chert-rich Dolomite with Large and Small Stromatolites	380
				LYTTELTON		Dark Chert-free Dolomite with Large Elongated Stromatolite Mounds	150
				MONTE CHRISTO		Light-coloured Recrystallised Dolomite with Abundant Chert; Stromatolitic; Basal Portion is Oolitic	700
				OAKTREE		Dolomite progressively Becoming Darker in Upper Portion; Chocolate-coloured Weathering	200
		BLACK REEF QUARTZITE		Shale Quartzite Arkosic Grit	25 - 30		

Figure 5: Stratigraphy of the North West dolomitic sequence (Eriksson et al., 2006)

2.4.2. Local geology

Light coloured chert-rich dolomites and oolitic chert outcrops were noted in the study area. The study area falls within the Monte Christo Formation which is a chert-rich Formation of Malmani dolomite (Figure 6). Monte Christo formation is about 700m thick but at Lichtenburg units is at 31.3 m (Eriksson et al., 2006).

The southern side of the C31A quaternary catchment is characterised by chert and tuff outcrops with greywacke and calcrete outcrops near Boikhutso (Figure 6). Diamictite, shale and mudstone outcrops are also dominant in the southern side of the catchment. The start of the Lichtenburg dolomitic compartment is characterised by the dark coloured dolomite of the Oaktree Formation (Barnard, 2000; Eriksson et al., 2006). The dark coloured dolomite is overlain by the chert-rich dolomite with interbedded oolitic chert of the Monte Christo Formation. The Monte Christo Formation is overlain by the dark chert-free dolomite of the Lyttelton Formation. The northern part of the catchment is characterised by the chert-rich dolomite of the Eccles Formation with chert breccia outcrops (Barnard, 2000; Eriksson et al., 2006).

Michaluk and Moen (1991) outlined the existence of the faults that are trending from east to west. These faults are notable in the Black Reef Formation and Chuniespoort Group which is east of Mafikeng. There are linear structures parallel to these faults that are recognizable from aerial photographs. These structures manifest as important magnetic lineament on magnetic survey and are associated with intrusion of dykes (Michaluk and Moen, 1991). Obbes (2001) has mapped many short faults found in the Monte Christo, Oaktree and Black Reef Formations.

The deposition of the Malmani Subgroup is onto the quartzite, conglomerate and shale associated with the Black Reef Formation. To the west and further south of Lichtenburg, this Subgroup lies on volcanic rocks of the Venterdorp Supergroup. A 5° low north dip angle is indicated on the geological maps of the Black Reef Formation (Meyer, 2014).

The Lichtenburg unit boundaries are formed by the Hendriksdal, Stryd and Elizabeth dykes and the southern boundary is formed by the Lichtenburg dyke (Obbes, 2001). Other dykes in this unit includes Zamekomst (N-S), Vlakplass (NW-SE), Paarl (E-W), Manana (N-S) and Lichtenburg (E-W) (Obbes, 2001).

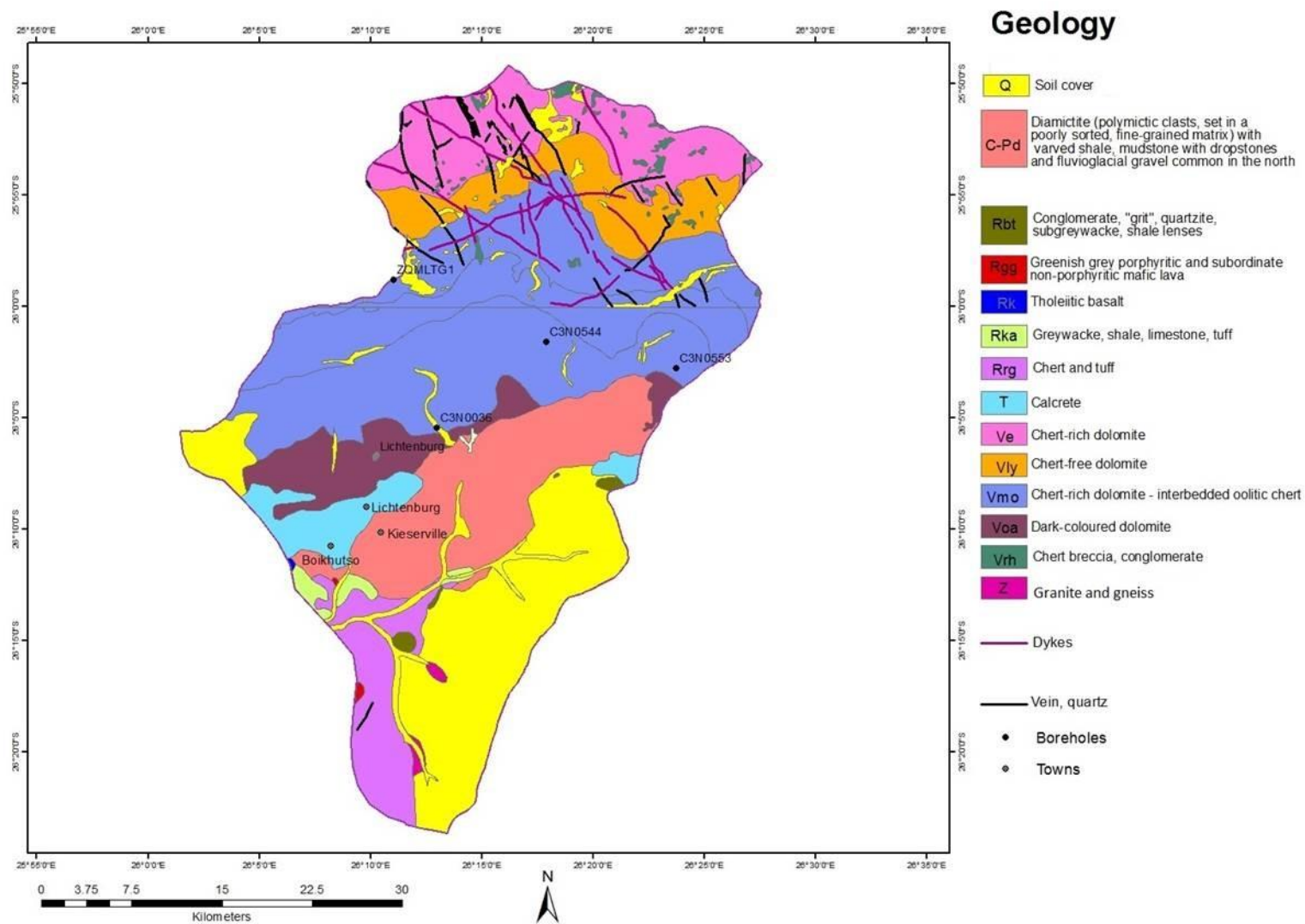


Figure 6: Geology of the study area with boreholes of interest (Modified for C31A quaternary catchment from Eriksson et al., 2006)

2.5. Hydrogeological settings

The Lichtenburg dolomite is described as a karst aquifer type according to the South African hydrogeological map series (DWA, 2001). This is as a result of groundwater occurrence in cavities dissolved in dolomites. Barnard (2000) stated that weak carbonic acid contained in rainwater infiltrates dolomite through joints, fractures and faults. The rainwater then dissolves dolomites through the following chemical reaction (Barnard, 2000):



(Dolomite) (Carbonic acid) (Calcium-bicarbonate) (Magnesium-bicarbonate)

Underground cavities have been dissolved in the past geological times mainly through the above chemical reaction (Bredenkamp, 2009). These cavities are connected across fractures and fissures to create an extensive interconnected or divided by impermeable dykes. These dykes penetrated the dolomite through separate compartments with distinctive hydraulic properties (Bredenkamp, 2009).

The study area is underlain by karstified dolomitic aquifer of the Chuniespoort Group (Malmani Subgroup). The boreholes yield in this area ranges from 0.5 l/s up to more than 5 l/s (Figure 8). This aquifer was classified as unconfined based on geological logs. The Malmani dolomite is regarded as one of the most important secondary aquifer in Southern Africa (Barnard, 2000). These aquifers are subdivided into compartments by dykes (DWAF, 2008). These dykes often act as a barrier to groundwater flow if not fractured (DWAF, 2008). These compartments are sometimes used for hydrogeological characterisation and also for groundwater management. Boundaries of the compartments are not completely impermeable; they are normally indicated by a noticeable change in groundwater levels (Barnard, 2000). These karst aquifers networks are often enlarged by dykes, weathering, solution features and the aquifer is controlled by the structure of the outcrop (Barnard, 2000).

Quantification of storativity (S) and transmissivity (T) was conducted in order to determine the abstraction schemes viability (Bredenkamp et al., 1991). Since the dolomitic aquifer was identified as a heterogeneous media and it was meaningless to apply average values of hydraulic parameters across the compartment (DWA, 2006).

In the Zeerust aquifer (Monte Christo Formation), a Transmissivity of 1200 m²/d was determined by Bredenkamp (1997). The Eccles Formation (chert-rich) Transmissivity was determined at 3000 m²/d for both the Grootfotein and Zeerust aquifers (Bredenkamp, 1997).

The underground flow sustains high yielding springs, which are situated at lower elevation of the surface of a compartment (Barnard, 2000). The compartment is usually closer to an impermeable boundary such as lithological contact or dyke. Groundwater is sometimes lost between compartments through leakage or overflow via dykes features, this occurs in low lying areas (Barnard, 2000).

Cogho (1982) mentioned that the hydraulic conductivity and primary porosity of dolomite is poor, however karstification and weathering in the Lichtenburg karst aquifer makes it a prolific aquifer. The Lichtenburg karst aquifer thickness of 31.3 m is a function of weathering and karstification (Cogho, 1982). Van Tonder et al. (1986) mentioned that the transmissivity value distribution is a function of severe heterogeneity of the weathered dolomite in the Lichtenburg karst aquifer. Based on the lithology report of ZQMLTG1 (Table 1), the Lichtenburg karst aquifer can be described as an unconfined aquifer.

Table 1: Lithology report for ZQMLTG1

Depth (mbgl)	Lithology
0-1	Soil
1-80	Dolomite

Barnard (2000) described the aquifer classification on a regional scale into four classes based on rock formations. The karst aquifer was defined as class C. 1230 boreholes yields were determined in the Chuniespoort Group in South Africa (Barnard, 2000). The aquifer yields presented in Figures 8, 9 and 10 were determined from the average yields of the 1230 boreholes. 5 types of borehole yields were determined into the following categories (Barnard, 2000); C1 (< 0.5 l/s), C2 (0.1-0.5 l/s), C3 (0.5-2 l/s), C4 (2-5 l/s) and C5 (> 5 l/s).

The mapping of aquifer yields was achieved by superimposing a grid over the lithology based hydrogeological units (Barnard, 2000). Each grid block dimension was set at one-sixtieth of a degree (one minutes or 1700 m by 1700 m). Each grid was colour coded according to the range

of borehole yield represented by the median borehole yield occurring at that particular grid block. Regional trends and patterns were selected based on visual inspection. This was supported by sufficient evidence and reasoning based on experience and extrapolated into areas of data scarcity (Barnard, 2000).

On a local scale, five boreholes within the Lichtenburg karst aquifer with yields were available on NGA. The borehole yields ranges from 0.02 to 1.83 l/s (0.02 l/s, 0.26 l/s, 0.85 l/s, 1.28 l/s and 1.83 l/s) with an average borehole yield of 0.85 l/s. The estimated borehole yields map is presented in Figure 11. A 2500 m grid was applied to all five boreholes in order to construct the yields presented in Figure 11. Inverse distance weighting interpolation based on spatial analysis was applied over the 2500 m.

The yield of the boreholes differs based on the host rock and transmissivity (Barnard, 2000). Holland (2012) stated that the potential of an aquifer to transmit groundwater is determined by the transmissivity. Therefore geological, topographical setting and dykes influences aquifer productivity. High density dolerite dykes influences the yield of an aquifer as they reduce transmissivity (Holland, 2012). Aquifers with densely packed dolerite dykes and low yield could be an indication of dykes acting as a barrier to the flow of groundwater (Holland, 2012). The illustrated dykes in Figures 8 and 9 are associated with the C3 type of borehole yield compared to the C5 aquifer with no dykes. Bush (1989) also stated that dolerite dykes manifested aquifers have lower borehole yields compared to aquifers with less dykes.

The vertical scale from Figure 9 and 10 is as follow; 1cm: 500 m. The vertical exaggeration factor of 10 was determined for Figure 9 and Figure 10. Dykes encountered are presented in Figure 9 and are related with a low yield aquifer in the study area. Meyer (2014) stated that these dykes are usually weathered near surface and allow groundwater flow and at depth they are thought to be impermeable.

Groundwater flow direction is presented in Figure 7. Groundwater flow is towards the north-eastern side of this aquifer. The hydraulic gradient (i) was calculated to be 0.0010 and this suggests a nearly flat groundwater gradient. X-Y-Z coordinates system was used to plot groundwater flow direction on excel based software.

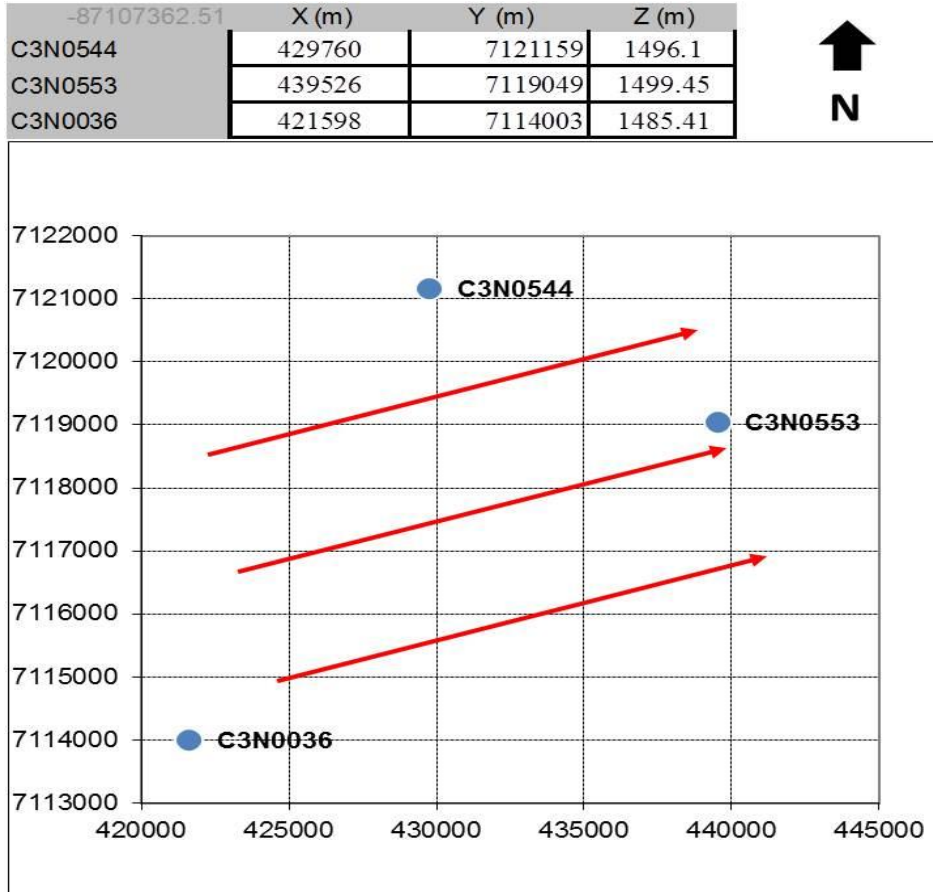


Figure 7: Groundwater flow direction

From Figure 9 and 10, potentiometric surface on table 3 were used to connect the groundwater table presented. Assumption was made that the aquifer is uniformly fractured in order to construct the cross section. In Figure 9, the potentiometric surface was lowered after the dykes with an assumption that large abstraction (28 million m³/a) in that region will lower the water table and a no flow boundary was assumed.

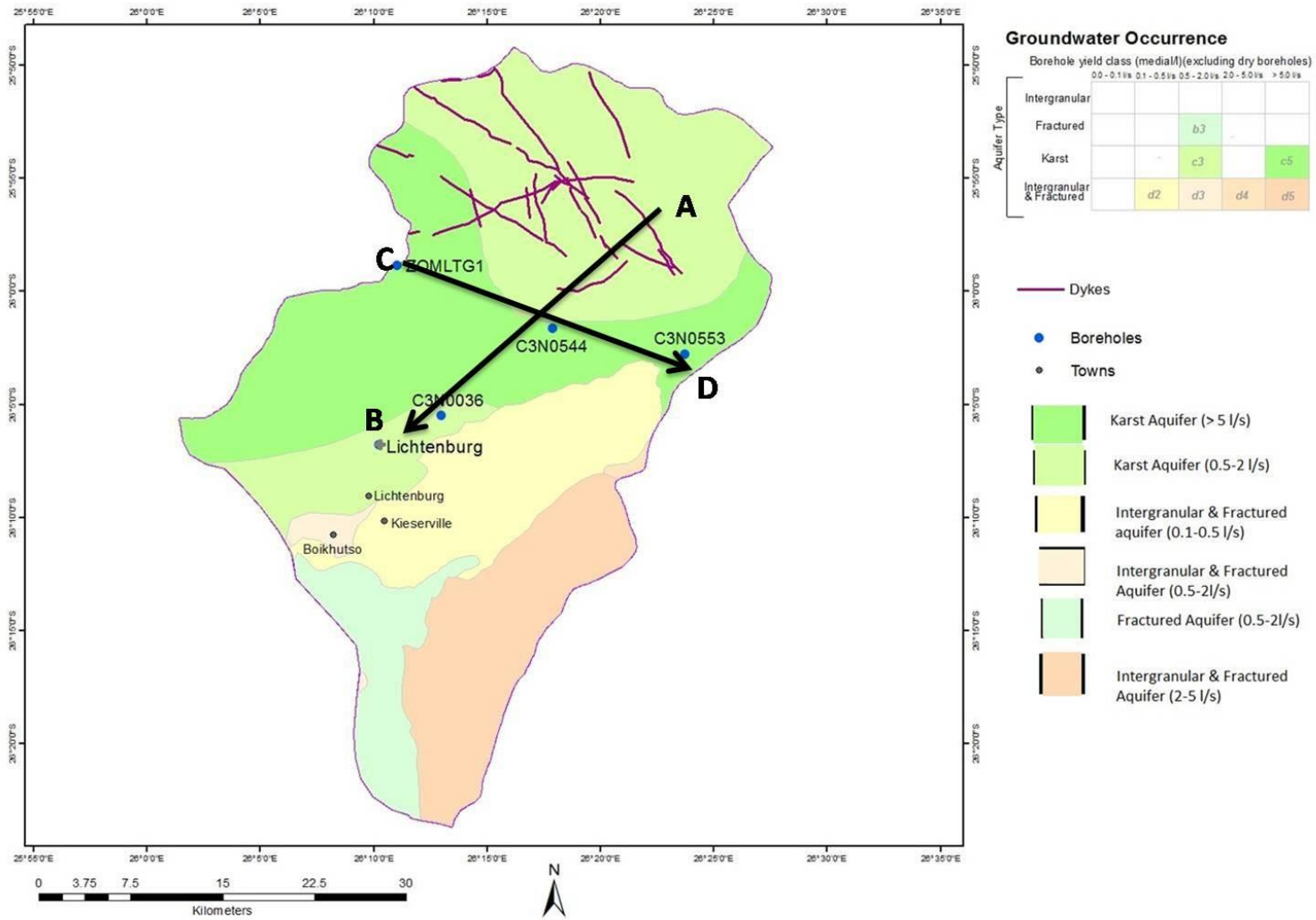


Figure 8: Aquifer map of the study area (Modified for C31A quaternary catchment from Barnard, 2000), with arrows showing cross sections lines.

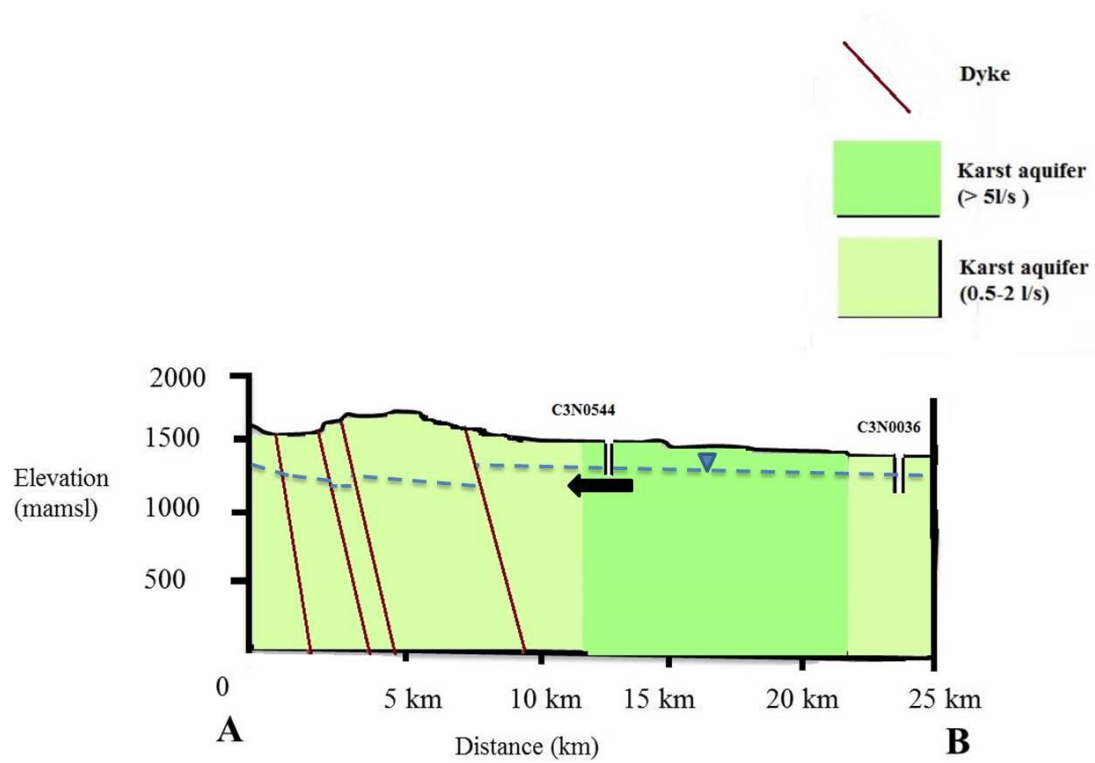


Figure 9: Hydrogeological Cross-section A-B (Modified from Barnard, 2000), with arrow indicating groundwater flow direction (hydraulic gradient: 0.0010 and vertical exaggeration factor of 10)

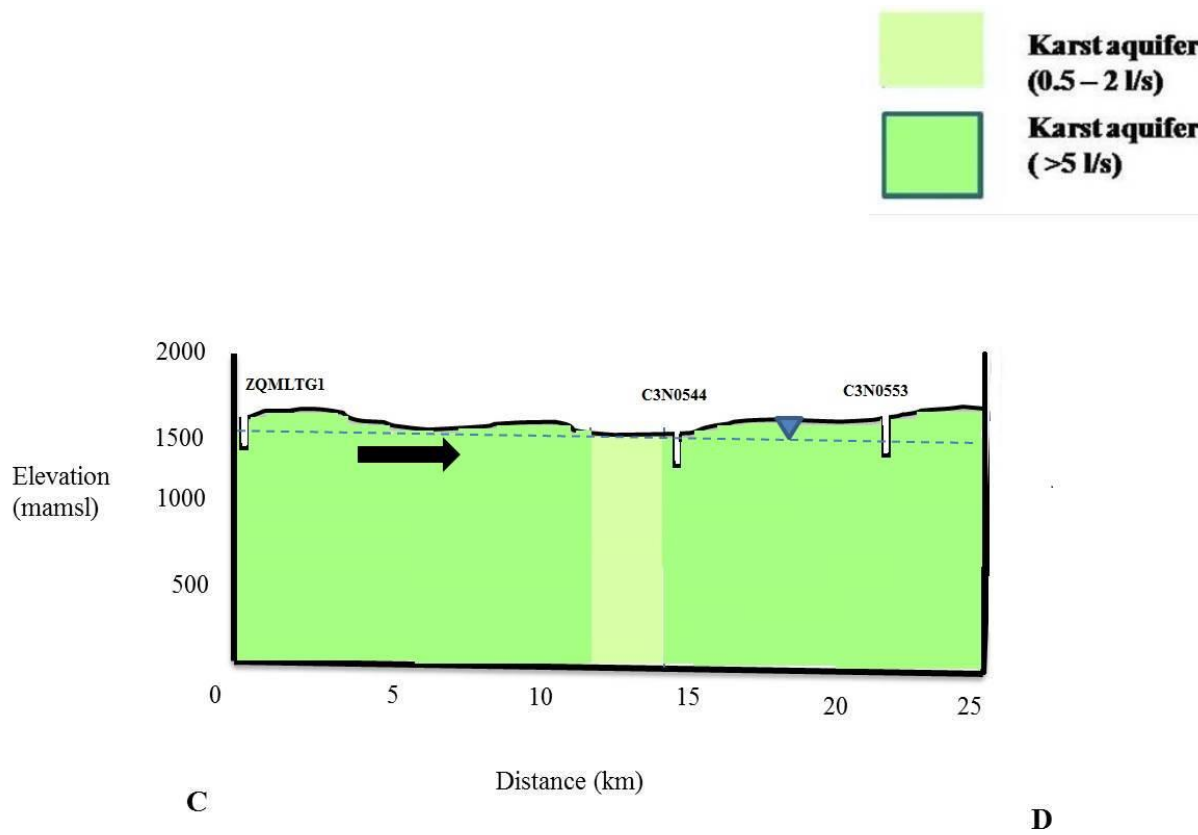


Figure 10: Hydrogeological Cross-section C-D (Modified from the Barnard, 2000), with arrow indicating groundwater flow direction (hydraulic gradient: 0.0010 and vertical exaggeration factor of 10)

Borehole yield map

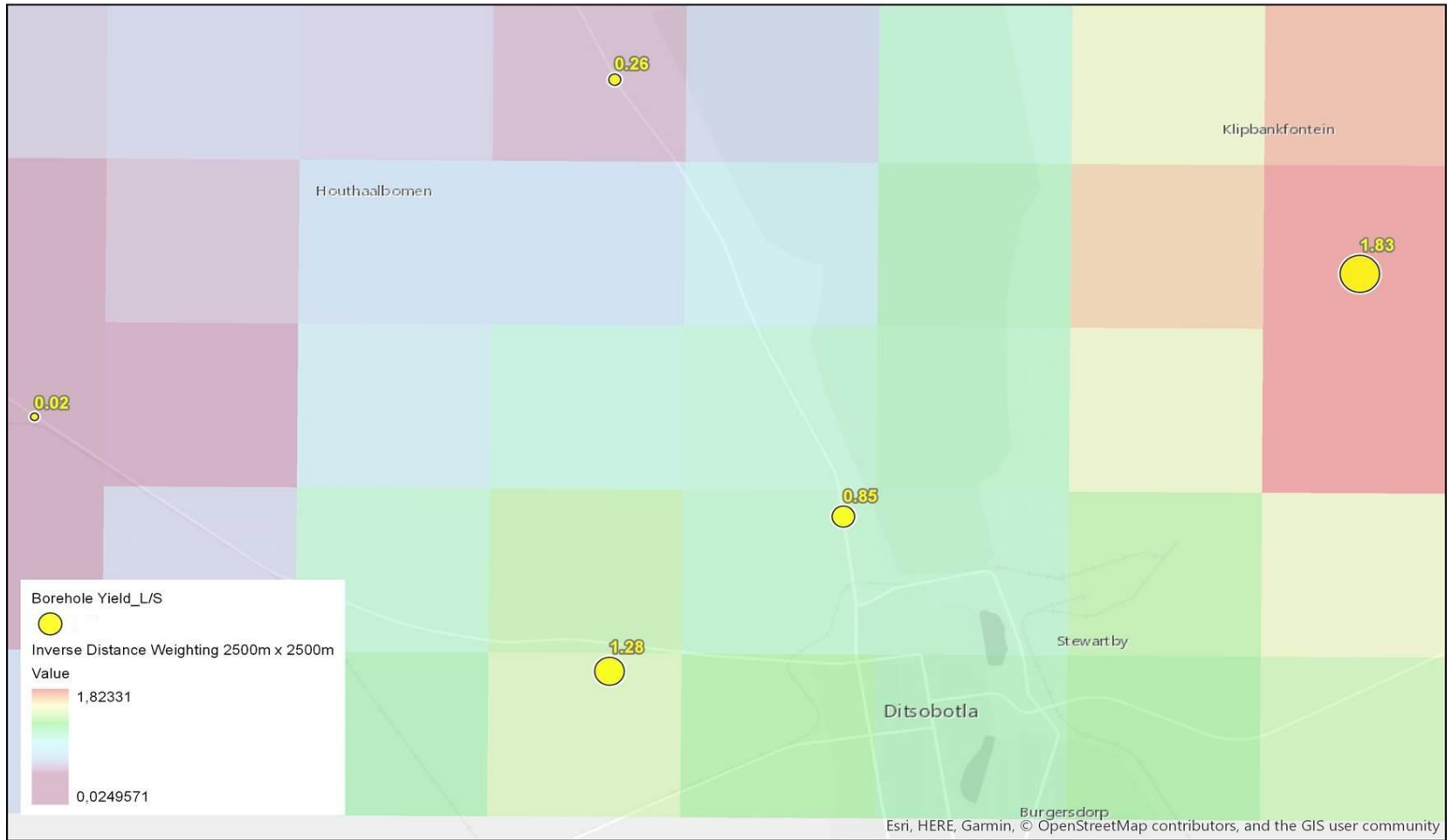


Figure 11: Local scale borehole yield map

Chapter 3: Literature review

3.1. Introduction

This literature review is focused on understanding the basic concepts of groundwater assessment in dolomitic aquifers. The relationship between groundwater level fluctuations, climatic variation and recharge will also be discussed. Various methods of groundwater assessment that correlates or are applicable in this study will be briefly discussed.

Assessment of groundwater resources in dolomitic aquifer is very interesting and was done in different regions in South Africa. Most assessments were conducted to investigate issues such as over abstraction, groundwater allocations, pollution as well as sinkholes. These dolomitic aquifers are part of important aquifers of the country as they often have a high borehole yield as well as good natural water quality (Barnard, 2000). The North West dolomitic aquifers are largely used for irrigation and public water supply (DWAF, 2008).

Climatic variation and recharge form a big part of groundwater assessment, especially in dolomitic aquifers. DWA has been conducting monitoring of groundwater levels and quality in dolomitic areas in South Africa as a special monitoring program over the years. Different recharge estimations have been made in the dolomitic areas by different authors.

3.2. El Nino- Southern Oscillation (ENSO)

Felix et al. (2015) defined El Nino as a periodic climate event associated with warm sea surface temperature in central and eastern tropical Pacific Ocean, which in turn has an impact on local weather. This generally increases the risk of drought at a global scale. UNDP (2017) stated that the El Nino event in 2015-16 was one of the strongest according to their record. It affected over 60 million people in 40 countries. There were massive floods, outbreak of diseases and some water sources dried up (UNDP, 2017).

El Nino started around April 2015 and was felt strongly around December as there was a disruption in rainfall and temperature. Most regions experienced weather anomalies and climate extremes (UNDP, 2017). In 1992 (El Nino year) only 12 tropical cyclones formed as compared to 16 in 2015.

3.2.1. El Nino in Southern Africa

El Nino generally causes drought in Southern Africa and decreases crop production. El Nino is traditionally associated with below average rainfall in Southern Africa and recent major drought was clearly associated with El Nino (Felix et al., 2015).

A moderate drought was experienced in 1991-92 and had a huge negative impact on crop production. A strong El Nino occurred in 1997-98 resulted in severe drought in most part of Southern Africa and caused a number of fatalities (Felix et al., 2015; UNDP, 2017).

Another El Nino event that occurred in 2002-03 resulted in severe drought in South Africa and Botswana. Many countries in the Southern Africa region were affected by the 2015 drought (Felix et al., 2015). Figure 12 below illustrate the mean annual precipitation as well as maximum and minimum temperatures of a station with historical data in the Study area.

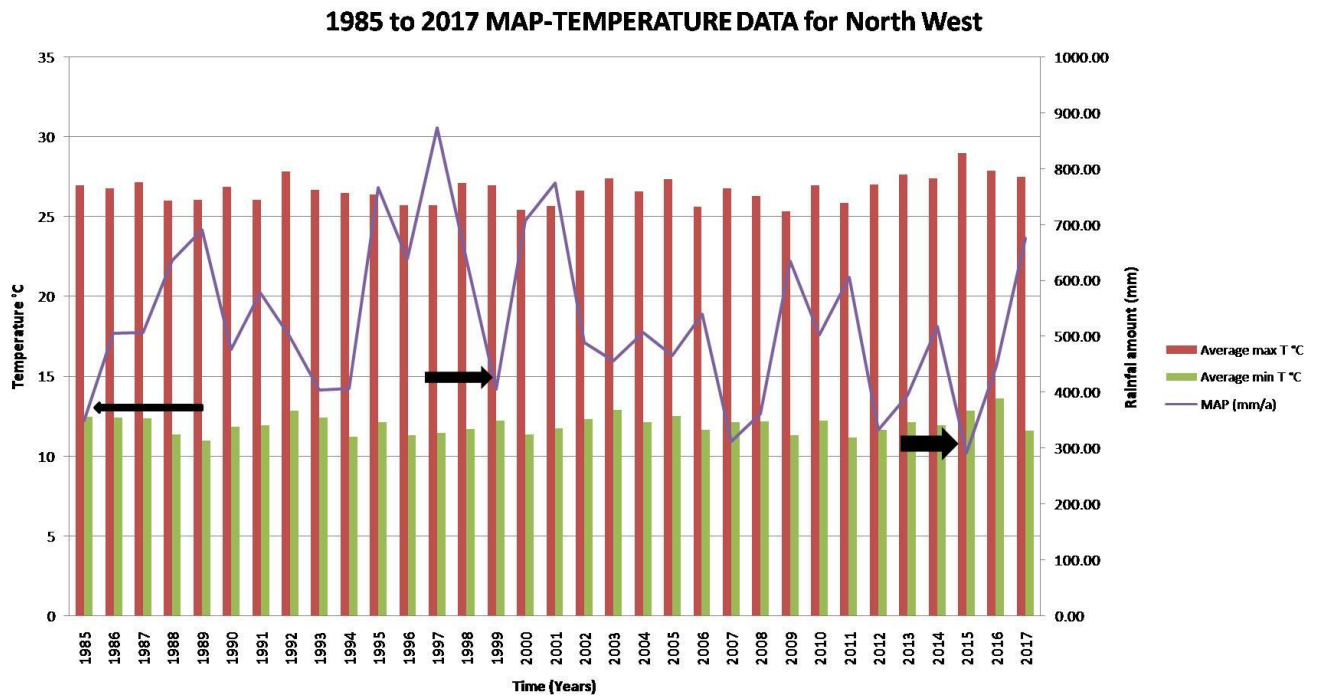


Figure 12: 1985 to 2017 North West MAP-Temperature data (Source of data: SAWS, 2017), with arrows indicating past El Nino events (Source of data: UNDP, 2017)

3.3. Aridity conditions in Southern Africa

The possibility of rainfall to recharge groundwater in arid and semi-arid region is very low (Beekman Xu and, 2003). Due to the arid and semi-arid conditions, hydrological drought is a common phenomenon in this region and this has a huge impact on water supply and irrigation. Groundwater recharge could be as little as 1% of annual rainfall during hydrological drought (Braune and Xu, 2008).

Mckee et al. (1993) stated that the standardized precipitation index (SPI) method is important in terms of assessing the extent of aridity. This method only requires potential evapotranspiration and precipitation data and has the capability to assess the duration as well as the intensity of drought (Masih et al., 2014). From Figure 14, the green shading represents unusually wet conditions and the red shading indicates dry conditions. It can be noted that Southern African region is under the impact of dry conditions from the 2015 SPI and these conditions are associated with low rainfall index (Abiye, 2016).

ARC (2016) classified the 2016 SPI in the study area as “mild drought”. The SPI of 2017 for the study area was classified as “moderately wet” (ARC, 2017). The calculations were based on a 12 months period.

Figure 13 below presents the aridity conditions in Southern Africa and also the aridity of the study area. Masih et al. (2014) stated that countries in the semi-arid regions are the most vulnerable to drought owing to excessive climatic variability.

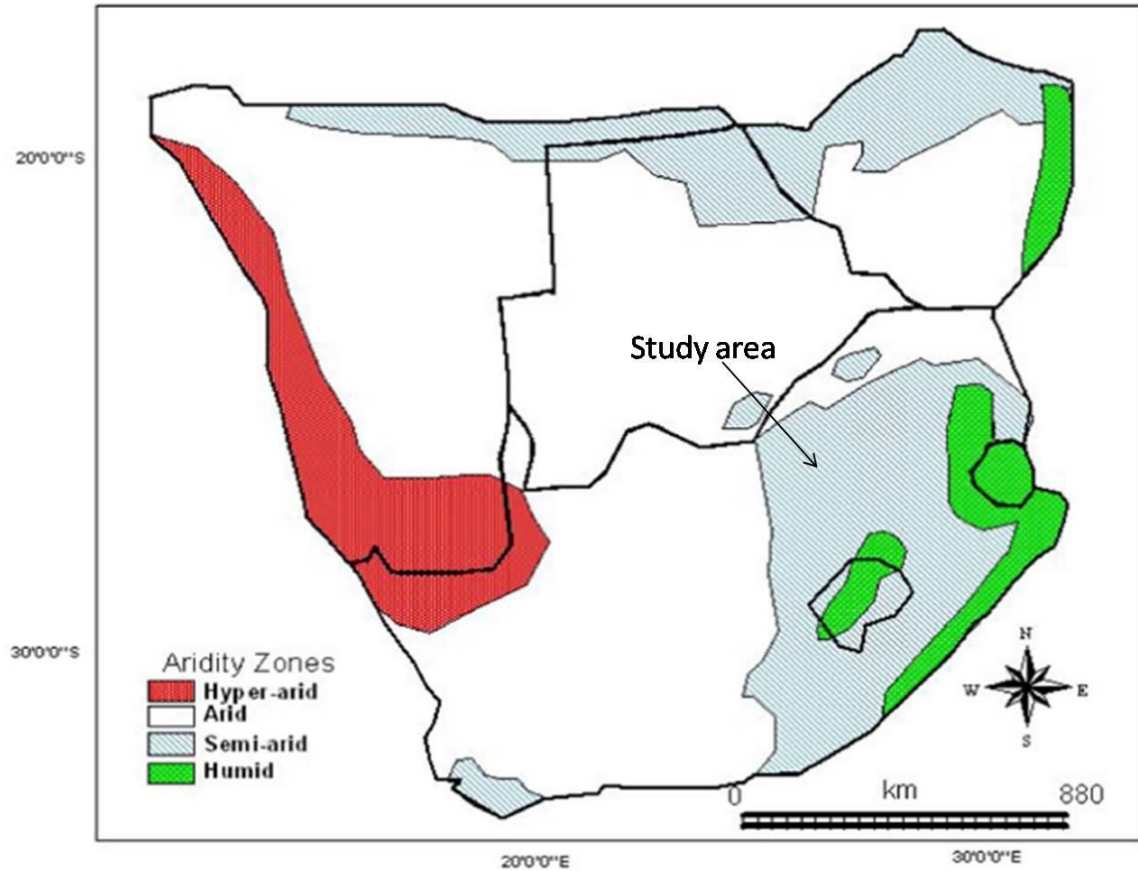


Figure 13: Aridity conditions in Southern Africa (Adopted from Abiye, 2016)

The SPI was in the negative category in central, Southern and Eastern parts of South Africa (Figure 14). This negative SPI indicate that the effective rainfall could decrease and this could lead to a decrease in groundwater recharge (Abiye, 2016).

Abiye (2016) stated that negative SPI in this region could aggravate salinity in shallow groundwater as results of strong evapotranspiration and also chloride from ocean water.

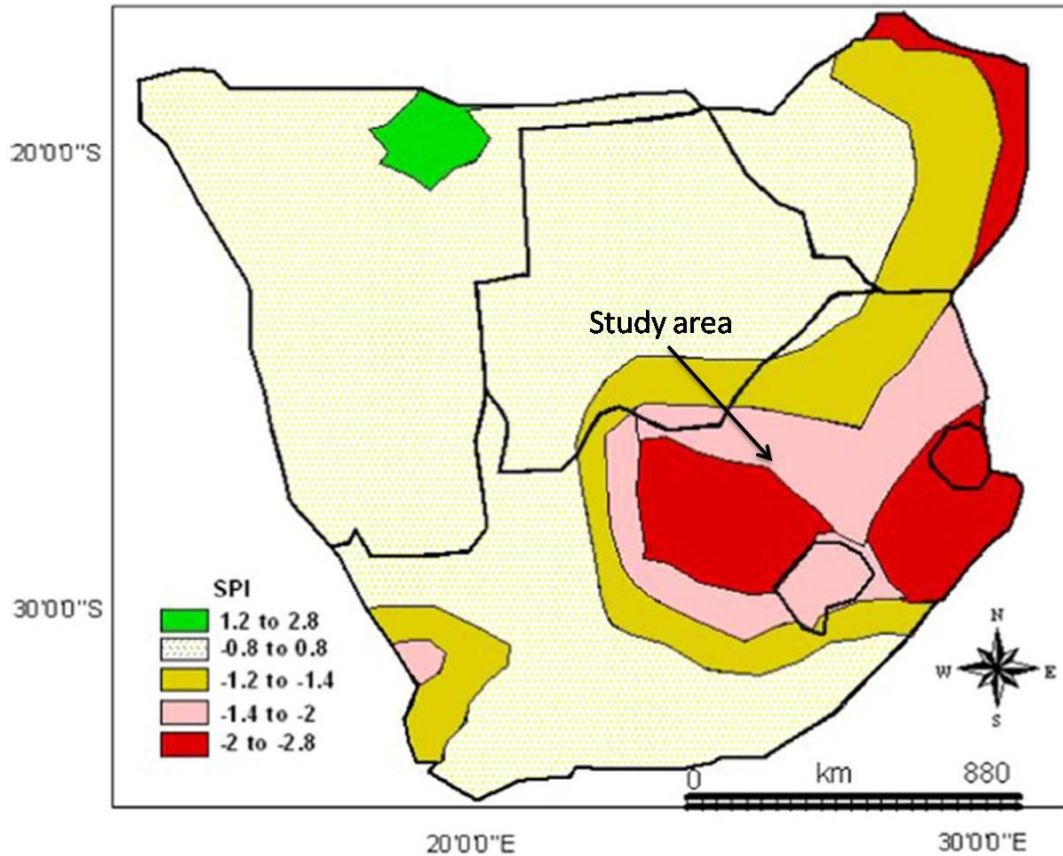


Figure 14: March 2015 to February 2016 standardized precipitation index (Adopted from Abiye, 2016)

Meyer (2005) determined that there is a strong correlation between groundwater levels and SPI values over a period of 40 years. A rise in groundwater levels was noticed during high SPI period (wet years). A decline in groundwater levels was observed during low SPI period (dry years). In order for effective recharge to occur, the SPI value should be more than 2 (Meyer, 2005).

Previous study by Manatsa et al. (2008) discussed the droughts that occurred in Southern Africa between 1902 and 1992. The study identified droughts in Zimbabwe based on SPI estimation. The most extreme drought was identified as the 1991-1992 in Southern Africa. The study concluded that El Niño-Southern Oscillation cannot be used alone as a drought predictor.

Richard et al. (2001) analysed droughts in South Africa that occurred between 1950 and 1998. This study found out that the droughts between 1970 and 1988 were severe and covered a larger area than the 1950-1969 droughts. These droughts were attributed to the ENSO.

Rouault and Richard (2005) used SPI values of 1900 to 1999 and analysed droughts in Southern Africa. The ENSO condition was linked to 8 of the 12 droughts that occurred during that period. The study showed a strong relationship between ENSO and droughts in Southern Africa.

A study by Calow et al. (2010) focused on the 1991-1992 droughts in South Africa. This study indicated that the shallow groundwater was the most affected by the drought.

Masih et al. (2014) indicated that droughts have intensified in the last few decades in terms of their geospatial coverage, severity and frequency in Africa.

3.4. The impact of climatic variation on groundwater resources

Beekman and Xu (2003) stated that from past, current observations and future predictions of the climate, there is an indication that the rainfall patterns seems to be changing. Rainfall is the main factor determining recharge in groundwater. Decrease in the frequency, amount, intensity and duration of rainfall have a huge impact on the groundwater resource (quality and quantity). Surface water response to rainfall is much faster than the response of groundwater. In Southern Africa, a 20% less rainfall could mean a decrease of 80% of recharge (Beekman and Xu, 2003).

Singh and Kumar (2010) stated that variations in regional precipitation and temperature affect all features of the hydrological cycle. The quantity of water reaching the surface, infiltrating into groundwater, flow to rivers or evaporates, is determined by variations in temperature and precipitation. Components of the hydrological cycle are illustrated in Figure 15 below.

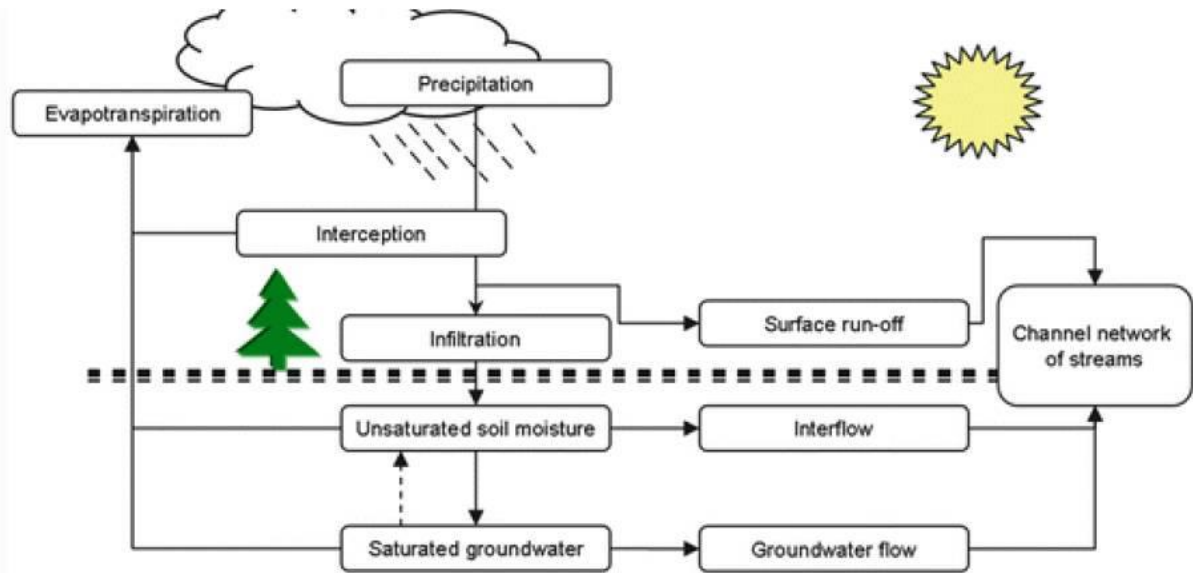


Figure 15: Illustration of the hydrological cycle (Source: Stagl et al., 2014)

Arora (2002) stated that precipitation and potential evaporation (available energy) in a region determines the annual runoff rates and mean annual evapotranspiration. The chances of runoff exceeding evapotranspiration if the available energy is low are very high for a provided quantity of precipitation. Runoff is likely to be a smaller fragment of precipitation if available energy is high, this will result in a high evapotranspiration (Arora, 2002).

Stagl et al. (2014) stated that spatial and temporal variations of the hydrological cycle as well as the site's physiographical condition determine the local hydrological condition. The potential of the atmosphere to hold moisture is enhanced by a rise in temperature leading to intensification of hydrological cycle (Stagl et al., 2014). Higher temperature will result in a decreased water vapour in the atmosphere. This will enhance actual evapotranspiration in areas where water is available. In areas with less precipitation this will increase the drought risk due to soil moisture reduction (Stagl et al., 2014).

Major alterations associated with climatic variability in the hydrological cycle include changes in seasonal distribution, duration and magnitude of rainfall as well as evapotranspiration. This could result in alterations in the water storage, soil moisture and surface runoff (Stagl et al., 2014).

Stagl et al. (2014) stated that when potential evapotranspiration is greater than the precipitation, the water balance will be negatively affected. The water balance will be positively affected if precipitation amount is greater than potential evapotranspiration and all physiographical conditions are favourable.

Groundwater is recharged by precipitation and also by surface water bodies (lakes and rivers) interaction. Climate change influences on surface water bodies and precipitation also affects the groundwater system (Singh and Kumar, 2010).

Kumar (2012) stated that due to warmer temperature associated with climate change, variation in rates of evaporation and precipitation will have a huge impact on the hydrological cycle. Variation in precipitation and temperature control the quantity of water that gets to the surface, transpire to the atmosphere and enters the groundwater system.

3.5. Concepts of groundwater assessment

3.5.1. Storativity and transmissivity

Bredenkamp (1995) stated that by estimating the mean storativity as well as aquifer thickness, the volume of groundwater stored in dolomitic aquifer may be estimated. It is also important to estimate the recharge in order to determine the storage. An average storativity value of between 1 and 5 % was suggested by Bredenkamp (1995) for dolomite aquifers in the North West dolomitic sequence.

Bredenkamp et al. (1974) and Bredenkamp (1987) determined storativity at the Bo Molopo area at 0.03 and 0.024, respectively. At the Grootfontein and Zeerust aquifers, Cogho (1982) and Botha (1993) determined storativity of between 0.025 and 0.05, respectively.

Bredenkamp (1993) also determined storativity at the Grootfontein aquifer based on chloride profiles in soil cover and CRD method at 0.023.

Bredenkamp (1997) determined Transmissivity of 1200 m²/d for both the Grootfontein and the Zeerust aquifers within the Monte Christo Formation. Transmissivity of 35 m²/d was determined by Bredenkamp (1997) for the Grootfontein aquifer in the Oaktree Formation.

Bredenkamp (1997) determined Transmissivity of 1100 m²/d for the Grootfontein aquifer in the Lyttelton Formation. In the Eccles Formation, a Transmissivity of 3000 m²/d was determined for both the Grootfontein and the Zeerust aquifers (Bredenkamp, 1997).

3.5.2. Groundwater recharge

Estimation of groundwater recharge gives an idea on how to manage groundwater resources efficiently. This is of importance in areas where there is a large demand of groundwater or where groundwater plays a vital role in social and economic development. Sun (2005) mentioned that estimating the rate of recharge in an aquifer is difficult compared to most assessment of groundwater resources.

Beekman et al. (1996) defined recharge as an addition of water to a groundwater reservoir. Recharge was also categorised four modes:

- Downwards flow of water through the unsaturated zone reaching the water table.
- Lateral and/or vertical inter-aquifer flow.
- Induced recharge from nearby surface water bodies resulting from groundwater abstraction.
- Artificial recharge such as from boreholes injection or man-made infiltration ponds.

According to Lerner et al. (1990) recharge can be categorized in three ways. These are:

- **Direct recharge-** direct infiltration of rainfall via an unsaturated zone to a body of groundwater.
- **Indirect recharge-** filtration to the water table through a riverbed
- **Localized recharge-** gathering of precipitation in water bodies in the surface, then percolation and infiltration through unsaturated zones to the groundwater body.

Recharge is controlled by entangled balance between several components of the hydrological cycle. These components include the following (Bredenkamp et al., 1995):

- Rainfall (intensity, variability, frequency and spatial distribution)
- Evapotranspirative losses (temperature, humidity and wind),
- Discharge losses (interflow, baseflow, springs, artificial discharge and lateral flow)
- Catchment (thickness, soil type, spatial distribution, topographical features and vegetation)
- Geology (rock types, structural geology and igneous intrusions)

According to Simmers (1988) there is no single estimation technique that does not give questionable results. Many methods can be used to estimate recharge but it is important to know that each method has limitations.

For the purpose of this study, chloride mass balance used by Bredekenkamp et al. (2009) will be of importance.

3.5.2.1. Chloride Mass Balance (CMB)

Chloride mass balance method revolves around a simple hypothesis of mass conservation between the addition of chloride flux in the subsurface and atmospheric chloride (Beekman et al., 1999). A profiling technique can be used to estimate the moisture flux in the unsaturated zone when piston flow is assumed, recharge can also be estimated by this technique. Due to the conservative nature of chloride, it can be used to estimate recharge in groundwater. The recharge equation as adopted from Eriksson and Khunakasem (1969) and also Houston (1988) is as follow:-

$$\text{Groundwater Recharge} = \frac{\text{Rainfall } \left(\frac{\text{mm}}{\text{a}}\right) \times \text{Chloride of rainfall } \left(\frac{\text{mg}}{\text{L}}\right)}{\text{Chloride of groundwater } \left(\frac{\text{mg}}{\text{L}}\right)} \text{ (mm/a)} \quad (2)$$

This method will not be suitable for areas with evaporites or where mixing with saline groundwater takes place. Rainfall from near the ocean contains variables of chloride content so it's advisable to be cautious when determining recharge using this method.

Abiye (2016) stated that it is not easy to determine an accurate proportion of recharge from rainfall as this doesn't consider the characteristics of the aquifer controlling percolation process and only relies on data sources and empirical methods.

After comparing the observations of previous studies, Abiye (2016) stated that the difference in recharge amount is determined by the quality of the data used which was measured (chloride deposit, both wet and dry deposition) rather than using data from literatures or extrapolation.

Abiye (2016) summarised proportion of recharge for CMB method as follows;

For rainfall < 500 mm/year = < 4% of MAP and for rainfall > 600 mm/year = up to 20% of MAP.

A number of authors used various methods to estimate recharge at dolomitic aquifers as follows;

Bredenkamp et al. (1964) estimated recharge at the Bo Molopo area at 5.3% (25-35mm) of MAP (566 mm/a) based on tritium profiles. This recharge value was underestimated. Bredenkamp (1993) also estimated recharge of 8.7% (49mm) of MAP (563 mm/a) at the Bo Molopo aquifer based on CRD method.

Cogho (1982) estimated recharge of 8.2% (46mm) of MAP (560mm/a). This was based on the simulation of the Grootfontein aquifer. The recharge was derived from soil moisture model, SVF, regression method as well as CMB.

Polivka (1987) estimated recharge of 13% (71mm) of MAP (MAP= 563mm/a) at the Bo Molopo aquifer based on CRD method.

Botha (1993) also estimated recharge of 4% to 22% (22 -123mm) of MAP (550mm/a) at the Zeerust area based on a groundwater model.

3.5.3. Groundwater quality

Bredenkamp (1995) stated that groundwater quality in the dolomitic sequence is generally good. Groundwater was classified as Ca-Mg-HCO₃, with EC less than 70 mS/m. Dolomitic groundwater complies with drinking water standards naturally, beside that the temporary hardness of the groundwater may cause insoluble carbonates deposition (Bredenkamp, 1995). One of the concerns raised was the groundwater pollution potential from the informal settlements

and also the impacts of irrigation. In some areas elevated nitrate were recorded and attributed to livestock waste and feeding creek.

3.5.4. Environmental isotopes

Meyer (2014) stated that oxygen-18 (^{18}O), deuterium (^2H) and tritium (^3H) are environmental isotopes that can be used to trace the origin of water resource. The linear relationship found when plotting $\delta^2\text{H}$ against $\delta^{18}\text{O}$ can be described by the following equation:-

$$\delta^2\text{H} = 8 \delta^{18}\text{O} + 10 \text{‰} \quad (3)$$

The equation above is called the Global Meteoric Water Line (GMWL), Craig (1961).

There is also another equation called the Pretoria Local Meteoric Water Line (LMWL)

$$\delta^2\text{H} = 6.7\delta^{18}\text{O} + 7.2 \text{‰} \quad (\text{IAEA-GNIP}) \quad (4)$$

3.6. Previous studies conducted in semi-arid regions and in karst environments

3.6.1. International studies

Panda et al. (2012): A total of 555 monitoring wells were used for this study from four different regions. The data used was from 1995 to 2005. In the semi-arid region of North Gujarat (NG), India, 180 wells were monitored four times each year. Monitoring of groundwater levels took place during pre-monsoon, monsoon, post-monsoon and during the water table recession stage. The North Gujarat aquifer is one of the most over-exploited aquifer in India. The study found out that the groundwater levels trend continues to decline in North Gujarat irrespective of seasons. This region experienced the biggest decline in groundwater table of 0.3 m/year (pre-monsoon) and 0.19 m/year (post-monsoon). There was an increase in both the intensity and frequency of rainfall during the monitoring period. The correlation between rainfall and groundwater levels of

pre-monsoon of the following year was found to be weak for arid and semi-arid regions. The study concluded that the integrated impact of climatic extremes and anthropogenic factors (over-abstraction) could be a major cause of the recorded decline in the water table.

Loaiciga (2003) studied the effect of climate change on recharge and groundwater use in a karst aquifer of Texas, USA. The study attributed the declining groundwater levels to both climate change and increased groundwater use. The study also found out that a rise in population and water demand will present a bigger threat on karst aquifers than climate change.

Bouchaou et al. (2011) investigated the impact of climate change on groundwater resources in the Souss-Massa basin, Morocco. The study determined that there has been a decrease in precipitation over the last 30 years. Groundwater levels observed indicated a declining trend during the same period. The decrease in recharge, recurrent droughts and increasing groundwater abstractions affected the groundwater level in the Souss-Massa basin. Isotopic and chemical tracers denoted a degradation of groundwater quality.

Nanekely et al. (2017) investigated the declining groundwater levels between 2006 and 2009 in the semi-arid region of Kurdistan, Iraq. The study determined that groundwater level decline was varying from 11 % to 88 % in this region. The average groundwater level decline was determined at 42 %. This study attributed the declining groundwater level to the combined impacts of dry periods, over-abstraction and the decrease in recharge.

3.6.2. Local studies

Bredenkamp (1964) determined the correlation between abstraction, groundwater levels of dolomitic aquifer and the average precipitation between 1958 and 1964. In 3 separate compartments, there was a steady decline in groundwater levels between 1958 and 1961 due to below average precipitation. The groundwater levels drastically recovered in 1961 after a good rainfall period. There was no conclusive proof that an increase in groundwater abstraction (number of boreholes increased) in the Blaauwbank area was directly affecting the groundwater levels and Grootfontein spring as abstraction data was insufficient.

Bredenkamp (1988) attributed the decline of the groundwater level in the Bo-molopo scheme to the serious drought between 1981 and 1988. Extensive pumping during period of low rainfall directly affected groundwater levels and spring flow.

Bredenkamp and Zwartz (1988) found out that there was groundwater levels fluctuation between 1978 and 1982. Continual decline of groundwater level were noted from mid-1982 to March 1988 and a total decline of 10 m was experienced. After the 1981 to 1988 drought, a recovery of groundwater level of up to 5 m was noted. This study concluded that the drought period affected the groundwater levels negatively.

Botha (1993) noted that excessive groundwater abstraction in the Rietpoort well scheme had a negative impact on the groundwater table. The Rietpoort spring became dry and this was during high rainfall season in 1993.

Bogare (2005)/ Report no: 22 (953) DWA investigated the declining of groundwater level from November 2004 to 2015. The Uitvalgrond well scheme failed during this period. The abstraction data was incomplete due to faulty meters. This study concluded that a threshold value of 65 mm per month was a cut of value for effective recharge.

Pyburn (2015) investigated the relationship between recharge, abstraction and spring flow in the Zeerust dolomitic aquifer. This study found that a large correlation between recharge, abstraction and spring flow/ groundwater level exist. The time-lag of 2-3 months between a recharge event and increase in spring flow/ groundwater level was determined. The reduction of spring flow/ groundwater level was attributed to over-abstraction and/or reduced recharge. The analytical model indicated a clear influence of abstraction on groundwater level around the Zeerust dolomitic aquifer.

Abiye et al. (2018) investigated the long term groundwater levels record in Johannesburg. This was conducted along with cumulative rainfall departure (CRD) method results. The study determined that groundwater levels are shallower in wetter conditions. This study concluded that

due to lack of correlation between groundwater level variation and rainfall, groundwater abstraction was assumed to be a possible cause of groundwater level fluctuation.

Chapter 4: Methodology

4.1. Desktop study

Previous studies have been reviewed and it will be useful in the data interpretation and comparison over different climatic conditions in the study area. Published and unpublished literatures were also reviewed.

Geological and hydrogeological maps were used for a full understanding of the geological and groundwater settings in the area.

4.2. Fieldwork

Different methods were used in order to achieve the main objectives of the study.

4.2.1. Groundwater level measurements

Three boreholes were selected in the study area for their uninterrupted historical data as well as access to their locations. The selected boreholes were C3N0036, C3N0544 and C3N0553 (Figure 23). The historical data is managed and audited by DWS on two database systems, NGA and HYDSTRA. Groundwater levels measurements were taken once every month on these boreholes using a dip meter and the same was done during site visit (Figure 16).

A standard field form was used to capture water level records as well as date, time and the name of the official. The captured groundwater levels, dates and times were uploaded in the two available databases of DWS. HYDSTRA was then used to process the data and produces data in form of trends or graphs for interpretations.

Other relevant information regarding the boreholes was captured during desktop study; this included coordinate, depth of boreholes, installed equipment, drilled date, lithology and all other parameters available.



Figure 16: Picture taken during measurement of groundwater level at C3N0036

4.2.2. Sampling and analysis

Groundwater sampling was conducted at two of the boreholes being monitored by DWS. The chosen boreholes were ZQMLTG1 (historical data for this borehole was available on WMS) and C3N0544. WMS is the groundwater quality database for DWS. Stable isotopes sampling was also conducted at this borehole during one of the site visits. Rainfall sample was also collected in the Lichtenburg area and analysed at UIS analytical services laboratory. For groundwater quality analysis, software called GW CHART (USGS) was used to plot a piper diagram. The piper diagram assisted in data interpretation in order to understand the overall behaviour of this aquifer.

4.2.2.1. Major ion chemistry

Historical groundwater quality data (1997-2016) for ZQMLTG were available for this area from the DWS database. The department has been monitoring major ion chemistry as well as metals at this borehole. Groundwater samples were collected using a 500 ml bottle inside a mobile cabin (Figure 17).



Figure 17: Sampling procedure used for major ion chemistry sampling

Bottles were marked and analysed for the above parameters. Before sampling took place, the boreholes were pumped for around 20 minutes. Field parameters such as temperature, electrical conductivity (EC) as well as PH were recorded on sites. Figure 18 below shows how field parameters and samples were taken after groundwater was pumped out of the borehole.



Figure 18: Field Parameters measurements on site

4.2.2.2. Environmental stable isotopes of ^{18}O and ^2H

Stable isotope ($\delta^{18}\text{O}$ and $\delta^2\text{H}$) were collected at the ZQMLTG1 borehole. This was done during the major ion sampling where the borehole was pumped for about 20 minutes before samples were taken. The bottle was well marked according to required standards and delivered to the University of the Witwatersrand, Hydrogeology Laboratory.

The LGR instrument was used for the analysis that operates on a laser system that contains an internal computer, liquid auto-sampler, a small membrane vacuum pump, and a room air intake line that passes air through a drierite column for moisture removal. 1 ml to 1.5 ml aliquot of a sample was pipetted into a 2 ml vial and closed with Polytetrafluoroethylene (PTFE) septum caps. A Hamilton microliter syringe was used to inject 0.75 μl of sample through a PTFE septum in the auto-sampler. The injection port of the auto-sampler was heated to 46°C to vaporize the sample under vacuum immediately upon injection. The vapour then travels down the transfer line into the pre-evacuated mirrored chamber for analysis. Five standards were used in the analysis procedure where the laser machine automatically calibrates itself and measures stable isotope values. The laser machine is known for providing acceptable results with a precision of approximately 1‰ for $\delta^2\text{H}$ and 0.2‰ for $\delta^{18}\text{O}$ in liquid water samples of up to at least 1000 mg/L dissolved salt concentration.

Chapter 5: Results and discussions

5.1. Recharge estimation using Chloride Mass Balance

Chloride concentrations in rainfall were estimated based on the MAP of 2016/17 hydrological year. Table 1 presents recharge estimated for 2016/17 hydrological year. Cl_{rain} and Cl_{gw} are one time values and not a mean for the hydrological year. Equation 1 was used to calculate recharge from C3N0544 data.

Table 2 below indicates recharge estimated based on the actual analysed Chloride concentration in rainfall from C3N0544.

Table 2: Recharge estimation based on sampled chloride concentration in rainfall (C3N0544)

Hydrological year	2016-17
Rainfall (mm/a)	702.8
Cl_{rain} (mg/l)	2.58
Cl_{gw} (mg/l)	12.9
Recharge (mm/a)	140.56
Recharge as % of rainfall	20 %

Recharge estimated based of CMB method indicated an annual recharge of 140.56 mm (20 % of MAP) for the 2016-17 hydrological year. The recharge correlates with Abiye (2016) who estimated recharge of up to 20 % of MAP if rainfall is greater than 600 mm/year. Groundwater levels picked up in the early months of 2017 and this is during the same period 20% (140.56 mm/a) of MAP (702.8 mm/a) recharge. The estimated recharge can be associated with the increased in groundwater levels noted in Figure 19 & 20. Weathering of the dolomite and the unconformity of the aquifer makes the Lichtenburg karst aquifer a highly recharged area.

5.2. Analysis of groundwater level trends against rainfall

Groundwater levels for 3 boreholes are tabulated below in Table 3. Historical trends are presented from Figure 19 to Figure 23.

Table 3: Summary of field measurements at all Groundwater level monitoring stations (Borehole depth: NGA)

Borehole ID	Co-ordinates	Date of measurement	Depth to bottom (m)	Elevation (mamsl)	Potentiometric surface (mbgl)
C3N0544	Lat: -26.0268 Long: 26.298	04/11/17	56	1520	23.90
C3N0553	Lat: -26.0463 Long: 26.3955	04/11/17	120	1533	33.55
C3N0036	Lat: -26.091 Long: 26.216	04/11/17	51	1514	28.59

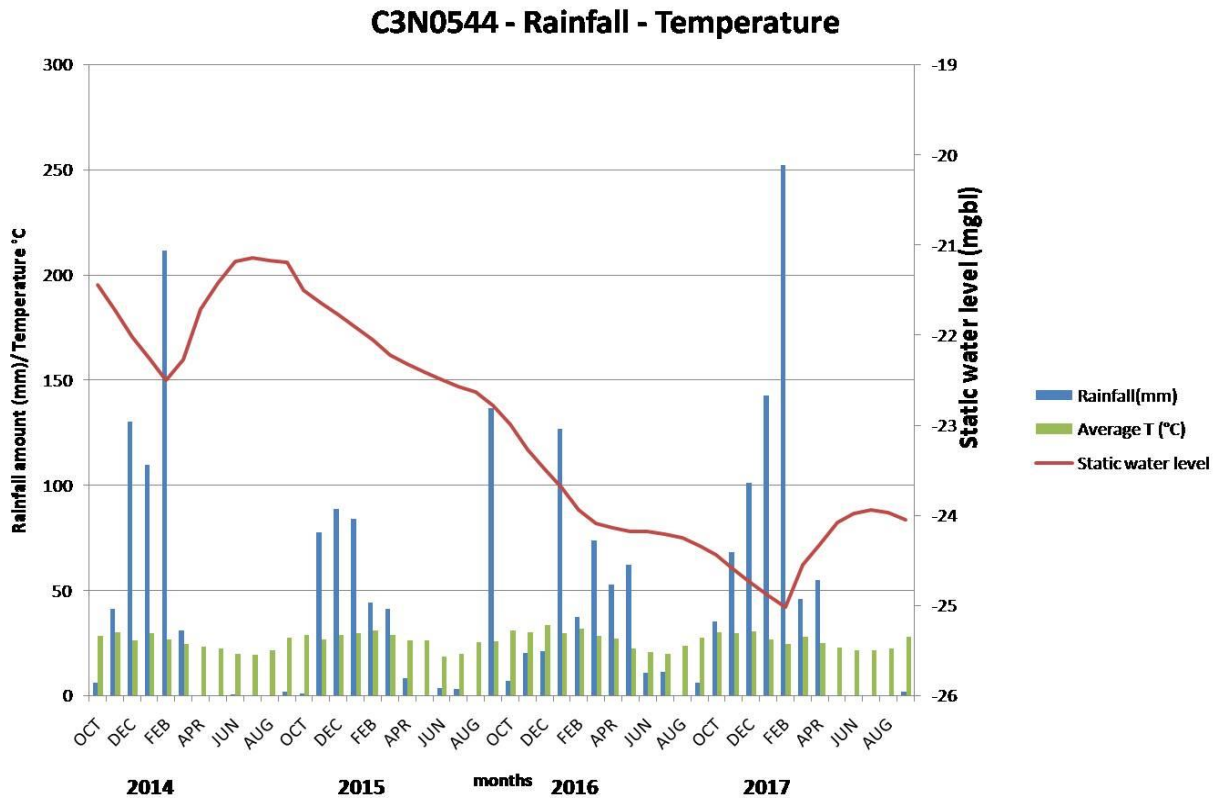


Figure 19: Relationship between groundwater levels (C3N0544), rainfall and temperature

C3N0544: This borehole is located approximately 17.35 km from the rainfall station. It belongs within a farming area where groundwater is the main source of water supply. There are two known production boreholes within 1km distance from this borehole. 1 borehole is being used for domestic water supply and the other for stock farming and both these boreholes are being pumped daily for several hours according to the owners. The rainfall sample was collected in this area and analysed for chloride and used in the CMB method.

Groundwater levels seem to respond to rainfall of over 200 mm per month as it is clear in February 2014 and also in February 2017 (Refer to a Figure 19). 200 mm per month seems to be a cut off value for an effective recharge to occur. There is a total decline in groundwater level of 4m between October 2014 and February 2017. This decline was experienced during the El Nino period associated with below average rainfall and high temperature. A negative SPI (-1.4 to -2:

Abiye, 2016) was calculated during the same period when the groundwater level was declining which means the possibilities of recharge was low.

A rise in groundwater level of 1m was noted between February 2017 and mid-2017 when the groundwater level continues to decline until the last measurements in 2017 (SPI: Moderately wet period; ARC, 2016). Besides those two months in 2013 and 2017, there is no correlation between rainfall and groundwater levels. The groundwater level is declining even during periods where recharge was estimated to be high. The only possible impact on groundwater level could be abstraction which is estimated to be about 37 million m³/a by DWS. The impacts of climatic variation and/or over-abstraction can be attributed to the 4m decline in groundwater level.

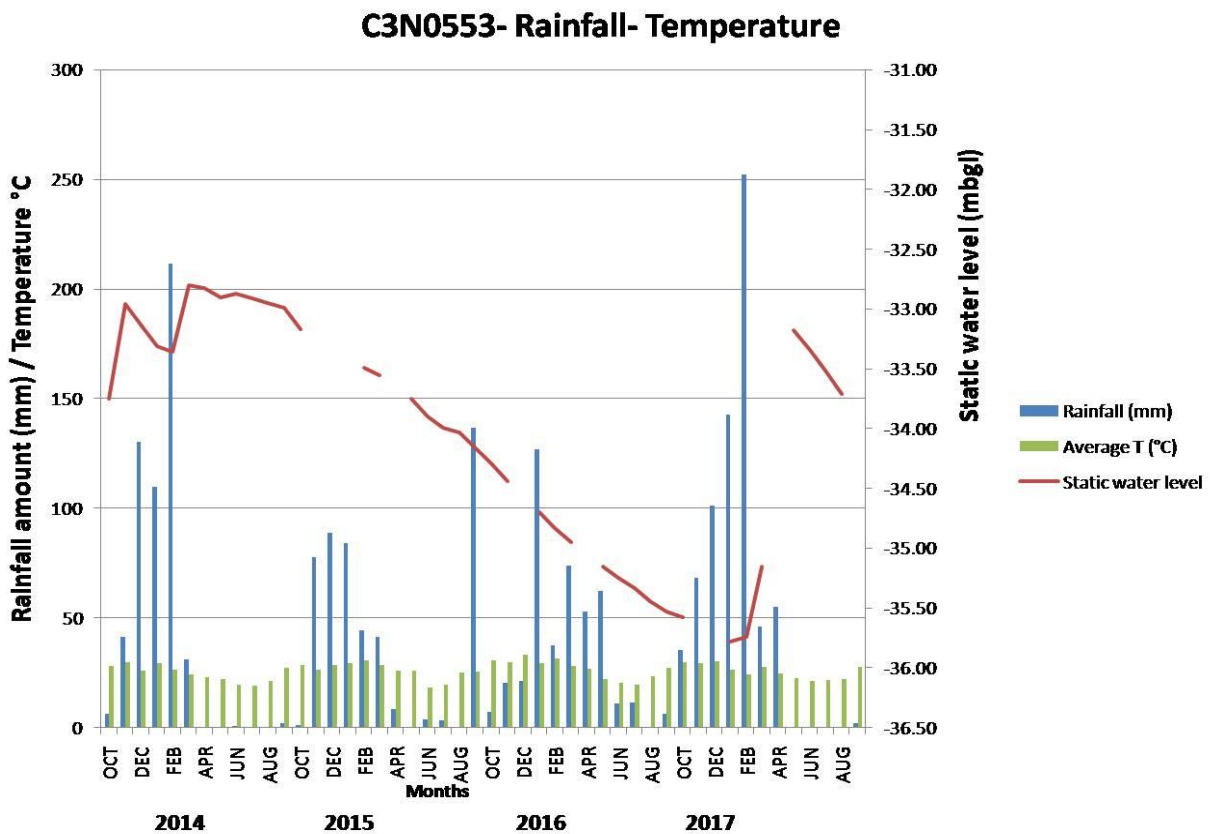


Figure 20: Relationship between groundwater levels (C3N0553), rainfall and temperature

C3N0553: This borehole is located approximately 24.8 km from the rainfall station. It belongs within an open farming area where groundwater is the main source of water supply.

As it was the case for C3N0544, the two rainfall events of over 200mm per month resulted in an immediate reaction of the groundwater level. There is a total decline of 2.9m in groundwater level between February 2014 and January 2017. The decline was during the El Nino period. A rise in groundwater level of 2.5m between February 2017 and May 2017 can be attributed to the 200mm rainfall event. The groundwater level continued to decline from mid-2017 until the end of 2017. The recharge was estimated at 20% of MAP (702.8 mm) and the groundwater level was still declining. The lack of correlation between rainfall and groundwater level can only suggest that abstraction could be another factor affecting the groundwater level.

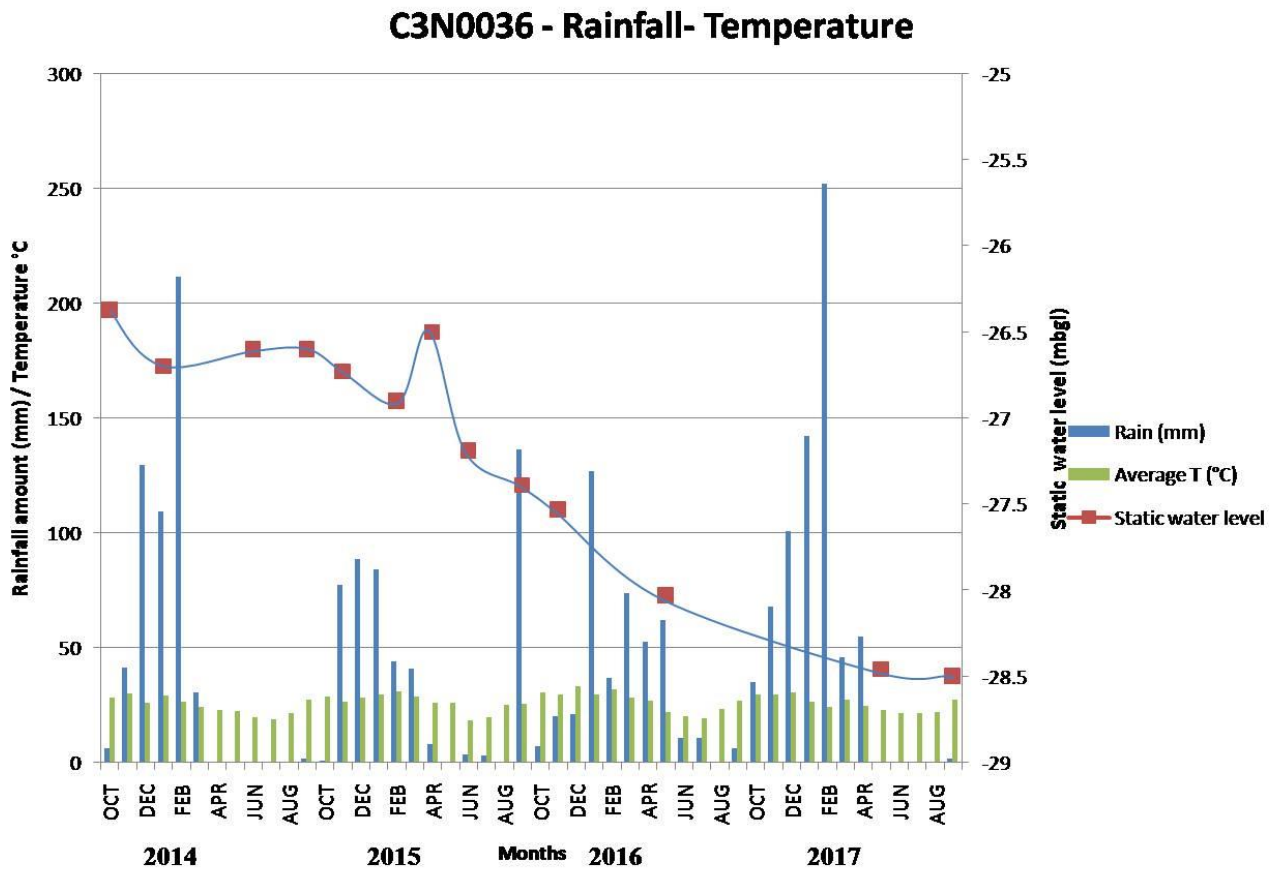


Figure 21: Relationship between groundwater levels (C3N0036), rainfall and temperature

C3N0036: This borehole is located approximately 6.9 km from the rainfall station used for this study. This borehole is located in an aquifer with a yield between 0.5 to 2 l/s and the other 2 boreholes yield is greater than 5 l/s.

Unlike the other two boreholes, this borehole did not respond to the 200 mm rainfall in February 2013 and February 2017. The only groundwater rise of 0.4 m was experienced in February 2015 and the rainfall was below 50 mm. A continual decline of groundwater table was experienced from March 2015 until the end of 2017. Groundwater continued to decline even after the El Nino period when rainfall was above average. There is no correlation between rainfall and groundwater level fluctuation. This borehole could be tapping a different aquifer.

From Figure 22 below, all boreholes are plotted together against rainfall and temperature. All boreholes experienced a decline during the El Nino period. Only C3N0036 behaved differently to the two other boreholes. All boreholes continued to decline until September 2017. The declining groundwater levels can be attributed to climatic variation and/or abstraction.

BOREHOLES-RAINFALL-TEMPERATURE

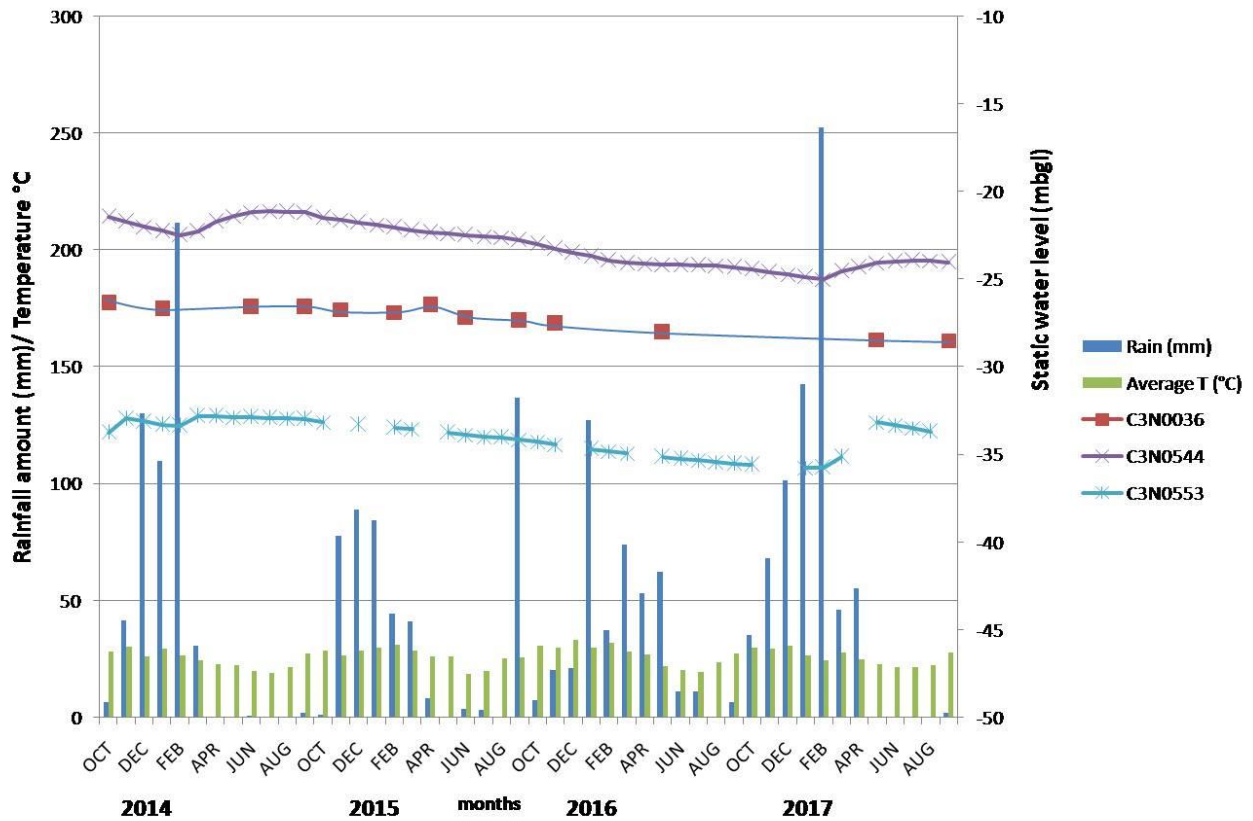


Figure 22: Four years period of groundwater level trends at three boreholes

The groundwater level fluctuations for all boreholes from 1990 to 2017 have been presented in Figure 23. A number of known droughts events as well as recharge events are also indicated. In the last 27 years of groundwater levels monitoring from this boreholes, arrow 1 in the figure indicate droughts events between 1991 and 1995. The total groundwater level decline for C3N0036 during the 5 year period was 4m and on average it was 0.8 m/year. The groundwater decline for C3N0544 was 5 m and an average of 1 m/year. C3N0553 groundwater declined was at 6 m and an average of 1.2 m/year. C3N0036 was the least affected by this drought period.

Period 28 Year 01/01/1990 to 01/01/2018

1990-2017

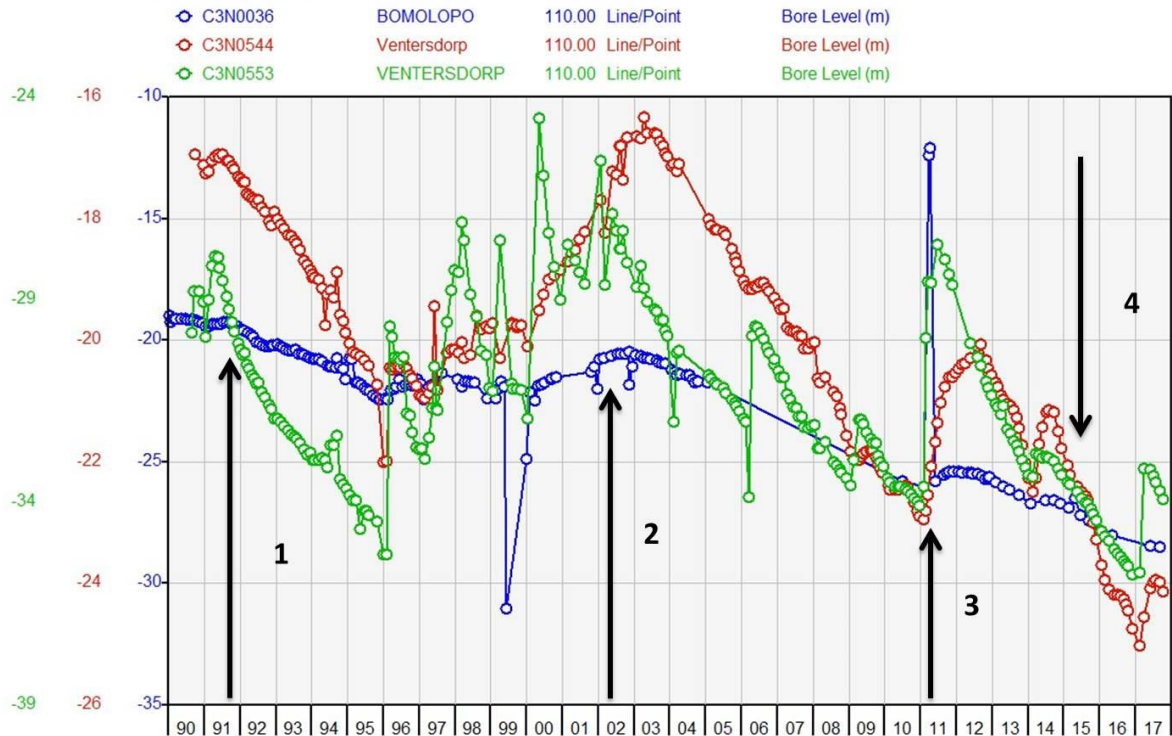


Figure 23: Groundwater level fluctuations from 1990 until 2017 with arrows indicating past drought events (HYDSTRA: DWS)

Arrow 2 represents the 2002 drought. The groundwater levels of all three boreholes continued to decline until 2011 despite rainfall seasons. C3N0036 was declining at the rate of 0.56 m/year, C3N0544 declining rate was at 0.72 m/y and C3N0553 experienced a decline of 1.63 m/year. Again C3N0036 was the least affected borehole.

The possible recharge event in this aquifer is indicated by arrow 3. All three boreholes experienced a sudden rise in the groundwater levels in early January 2011. The recharge of 2010/11 hydrological year was estimated at 37.3 % of MAP (835 mm/a), 534 mm was experienced just in 3 months before the peak. C3N0036 experienced a groundwater level increase of 14m in just 2 months. C3N0544 and C3N0553 experienced a groundwater level rise of 3 m and 4 m respectively. The Groundwater level continued to decline after that peak in 2011.

Due to compartmentalization in the karst aquifer, rapid groundwater level fluctuations are common. Groundwater rises rapidly during period of high recharge and decline rapidly during

low recharge and high abstraction period. Compartmentalization, weathered dolomite and the unconformity of this aquifer played a huge role in the rapid fluctuations of groundwater levels from the three observed boreholes.

The 2015 ENSO associated climatic variation is represented by arrow 4. Groundwater levels for all boreholes were declining continuously until January 2017. C3N0036 experienced the least groundwater decline of 0.75 m/year. C3N0544 and C3N0553 experienced groundwater decline at the rate of 2 m/year and 1.5 m/year respectively.

A recharge of 20 % of MAP (702.8 mm/a) was estimated for the 2016/17 hydrological year but the groundwater levels continued to decline. This is just an indication that climatic variability alone is not responsible for the declining groundwater table. A combination of abstraction and climatic variability can be attributed to the declining groundwater levels.

The location of the boreholes in respect to the rainfall station which rainfall data was collected from is presented in Figure 24.

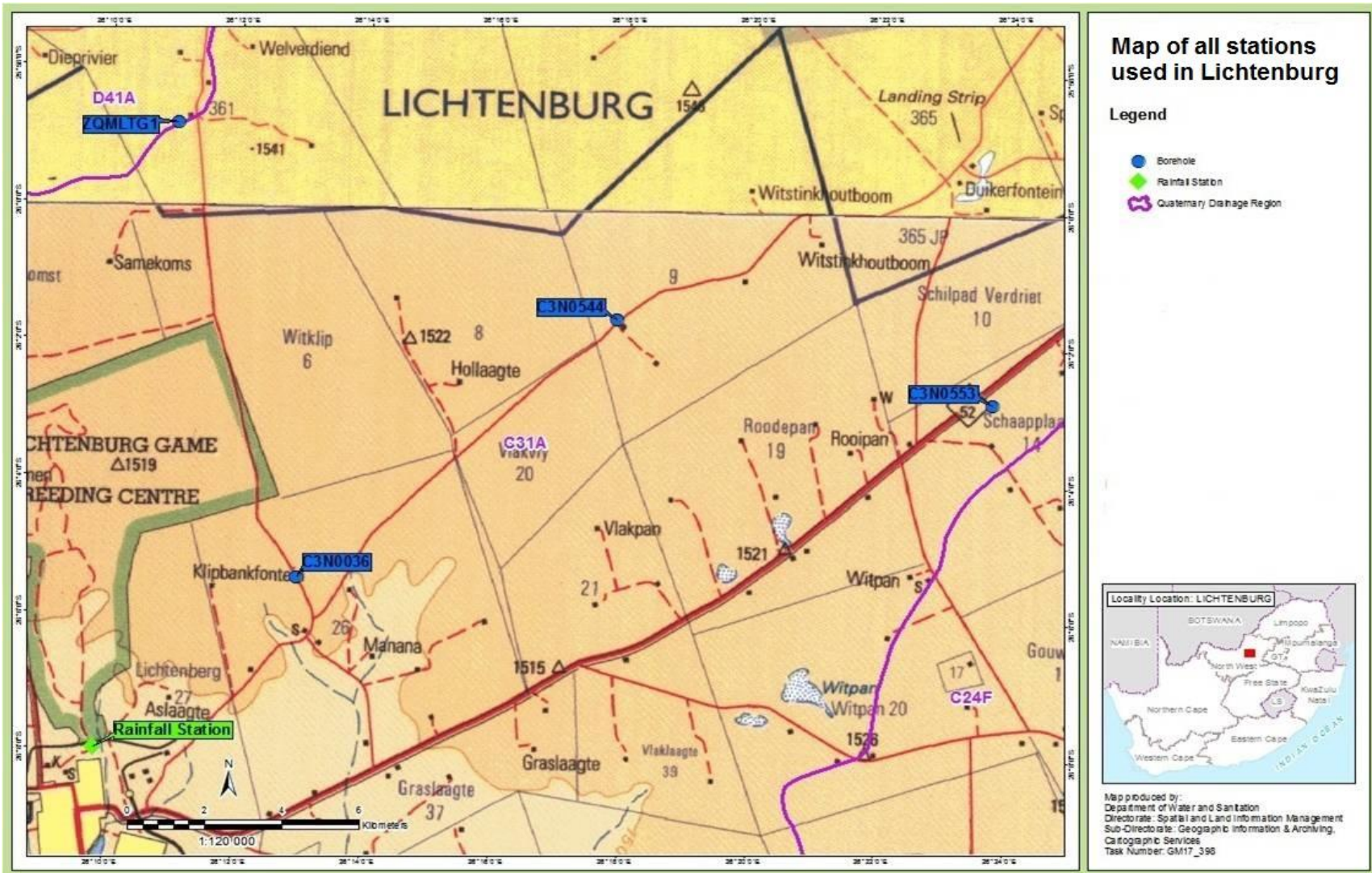


Figure 24: Boreholes location in respect to the rainfall station (Modified from DWS, 2006)

5.3. Field parameters analysis

Various methods were applied to measure and interpret groundwater quality data over varying climatic conditions in the study area. A groundwater quality monitoring station ZQMLTG1 was sampled for this purpose. The historical data as back as 1997 was available for this station. This borehole is equipped with a pump.

Table 4: Field details of groundwater quality monitoring station ZQMLTG1 (Source: NGA, DWS)

Borehole ID	Co-ordinates	Constructi on date	Elevation (mamsl)	Groundwater level (mbgl)	Depth to bottom (m)
ZQMLTG1	Lat: -25.9812 Long: 26.183	1997-11-18	1530	29.26	80

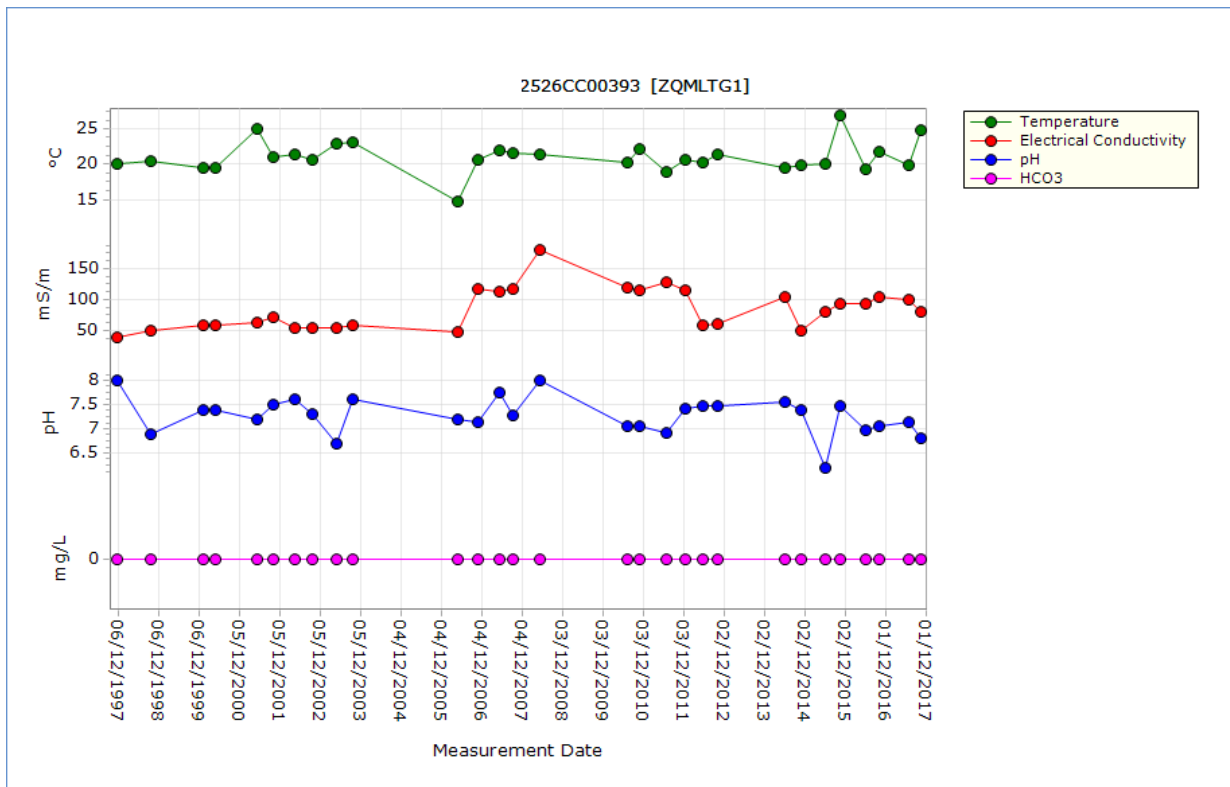


Figure 25: EC-pH trends over a period of 20 years (Data source: Chart, DWS)

In the Figure 25, it is clear that the pH is ranging from 7 and 8. Only in May 2003 and April 2015 pH was less than 7. In April 2005 and May 2003, pH in groundwater can be attributed to El Nino as it was around the same period of the El Nino in South Africa. There is no clear indication to conclude whether climatic variation resulted in the drop of pH. The pH in groundwater sampled in October 2016 was recorded at 7.46, so it is still between the historical values of between 7 and 8.

Electrical conductivity (EC) in groundwater was fluctuating between 40.3 and 179.5 mS/m since 1997. The highest EC concentration was recorded in 2008 and dropped back to around 60 mS/m in 2012. EC values fluctuated more after 2012 until the last sampling in 2017. Climatic variations didn't have any significant impact on the EC in the Lichtenburg karst aquifer. During the El Nino periods, pH in groundwater tends to drop as it was the case in 2003 and 2015.

Due to surface (soil) soil conditions during El Nino periods such as increased surface temperature, increased EC and reduced pH; interaction of precipitation with soil surface impact the groundwater conditions as indicated in figure 25. Increase in temperature, EC and a reduced pH can be attributed to recharge conditions during El Nino.

Table 5: Field measurement results for ZQMLTG1 (Source: NGA, DWS)

Date of measurements	EC (mS/m)	pH	Temperature (°C)
18/11/1997	40.3	8	20
14/09/1998	50	6.9	20.4
01/01/2000	58.6	7.4	19.6
19/04/2000	59.5	7.4	19.6
03/05/2001	64.5	7.2	25
04/10/2001	73	7.5	21
09/04/2002	55.6	7.6	21.4
20/09/2002	54.9	7.3	20.6
22/04/2003	55.1	6.7	22.9
18/09/2003	59.7	7.6	23.2
26/04/2006	49.2	7.2	14.8
19/10/2006	117.8	7.14	20.6
09/05/2007	114	7.74	22
04/09/2007	116.5	7.28	21.6
07/05/2008	179.5	8	21.4
10/07/2010	119.9	7.06	20.3
20/10/2010	115	7.06	22.2
30/06/2011	129	6.92	18.9
15/12/2011	115.6	7.43	20.7
24/05/2012	60.1	7.46	20.2
27/09/2012	60.9	7.46	21.4
28/05/2014	104.9	7.55	19.5
27/10/2014	51.5	7.38	19.9
26/05/2015	80	6.2	20.1
15/10/2015	94.9	7.46	26.9
02/06/2016	93	6.98	19.3
23/09/2016	104.2	7.05	21.8
26/06/2017	99.7	7.13	19.9

5.4. Laboratory parameters analysis

5.4.1. Major ion

Piper diagram was used to plot and analyse groundwater quality data from 1997 until 2017.

Table 6: Major ion composition (mg/l) for ZQMLTG1 (Source: DWS CHART)

Parameters	Ca	Mg	K	Na	TALK	Cl	SO4	TDS
Date								
Nov-97	61.1	35.3	0.66	3.3	296.8	3.4	4.4	478
Sep-98	63.7	33.4	0.59	3	290.4	3.3	2	468
Apr-00	63.367	34.711	0.599	3.72	302.442	5	2	486.341
May-01	65.762	33.114	0.617	4.176	286.963	5	2	468.727
Oct-01	47.837	45.968	0.649	3.162	285.985	5	5.422	463.834
Apr-02	66.321	37.051	0.642	3.396	293.428	5	6.136	484.314
Sep-02	63.439	35.636	0.499	2.524	295.163	5	9.585	484.702
Apr-03	64.147	36.885	0.662	2.81	296.267	5	4.106	483.433
Sep-03	66.854	35.921	0.555	2.664	307.725	5	5.256	500.835
Jun-04	60.287	38.389	0.693	3.595	288.195	6.416	3	471.702
Oct-04	65.481	37.179	0.659	3.458	297.554	5.006	3	485.767
May-05	62.041	36.265	0.661	3.391	301.441	2	2	482.811
Aug-05	62.616	35.049	0.711	2.96	294.864	6.877	2	478.58
Apr-06	60.97	35.075	0.737	3.255	286.312	4.451	2	464.236
Oct-06	63.757	34.903	0.561	3.105	291.103	6.405	2	474.711
May-07	62.602	35.926	0.77	3.216	293.996	7.897	9.777	487.845
Aug-07	62.42	36.557	0.748	3.526	293.293	5.267	4.494	480.302
Jul-10	75.571	38.42	1.36	4.66	395.001	6.77	3	*
Oct-10	69.929	34.156	1	5.554	233.25	9.036	3.534	432.913
Jun-11	44.331	34.975	1	2	234.51	5.092	1.5	399.454
Dec-11	61.591	33.381	2.185	4.538	281.663	6.437	1.5	480.394
May-12	70.865	35.701	2.082	2	287.689	5.423	1.5	491.99
Sep-12	72.535	31.704	2.827	*	277.217	*	3.011	*
May-14	56.667	37.704	*	*	326.169	4.833	1.5	*
Oct-14	68.594	35.804	*	*	303.101	7.508	3.839	*
May-15	77.51	*	1.392	1.5	306.983	8.602	4.019	*
Oct-15	80.321	33.853	3.6	*	326.392	*	1.5	*
Jun-16	69.6	37.7	1.1	3.3	300.3	8.7	0.6	509.69
Sep-16	45.1	31.7	3.7	16.3	272.7	7	5	456.904

*Parameters were not analysed

Laboratory results with missing data were not used for any analysis in this study. Ion balance results are tabulated in Table 7 below.

Iron balance is calculated using the following formula;

$$\text{Ion Balance} = \frac{\sum \text{Cations} - \sum \text{Anions}}{\sum \text{Cations} + \sum \text{Anions}} \times 100$$

(5)

Table 7: Ion balance from 2012 to 2016 (DWS CHART)

Date	Ion balance %
Nov-97	8.2
Sep-98	9.4
Apr-00	7.9
May-01	10.6
Oct-01	11.1
Apr-02	11.2
Sep-02	7.9
Apr-03	9.9
Sep-03	8.2
Jun-04	10.9
Oct-04	10.9
May-05	9.2
Aug-05	8.3
Apr-06	9.7
Oct-06	9.3
May-07	7.2
Aug-07	9.4
Jul-10	3.2
Oct-10	18
Jun-11	8.2
Dec-11	7.1
May-12	11.2
Sep-12	10.7
May-14	2.2
Oct-14	5.3
May-15	18.8
Oct-15	4.7
Jun-16	9.6
Sep-16	5.8

Some of the ion balances are greater than 5% and this indicate that some errors might have happened during sampling or analysis. Borehole C3N0544 was sampled in November 2017 and the results are tabulated in Table 8 below.

Table 8: Major ion results for C3N0544 (mg/l)

Parameter	Ca	Mg	K	Na	Talk	Cl	SO4	TDS
November 2017	63.8	26	0.53	3.53	249	12.9	7.6	442

Iron balance of this analysis was calculated at -0.63 %.

All major ion chemistry results have been plotted in Piper diagrams from Figure 26 to 27. The results with missing parameters were excluded from this analysis. This was done in order to determine the hydrogeological facies of the Lichtenburg dolomitic aquifer.

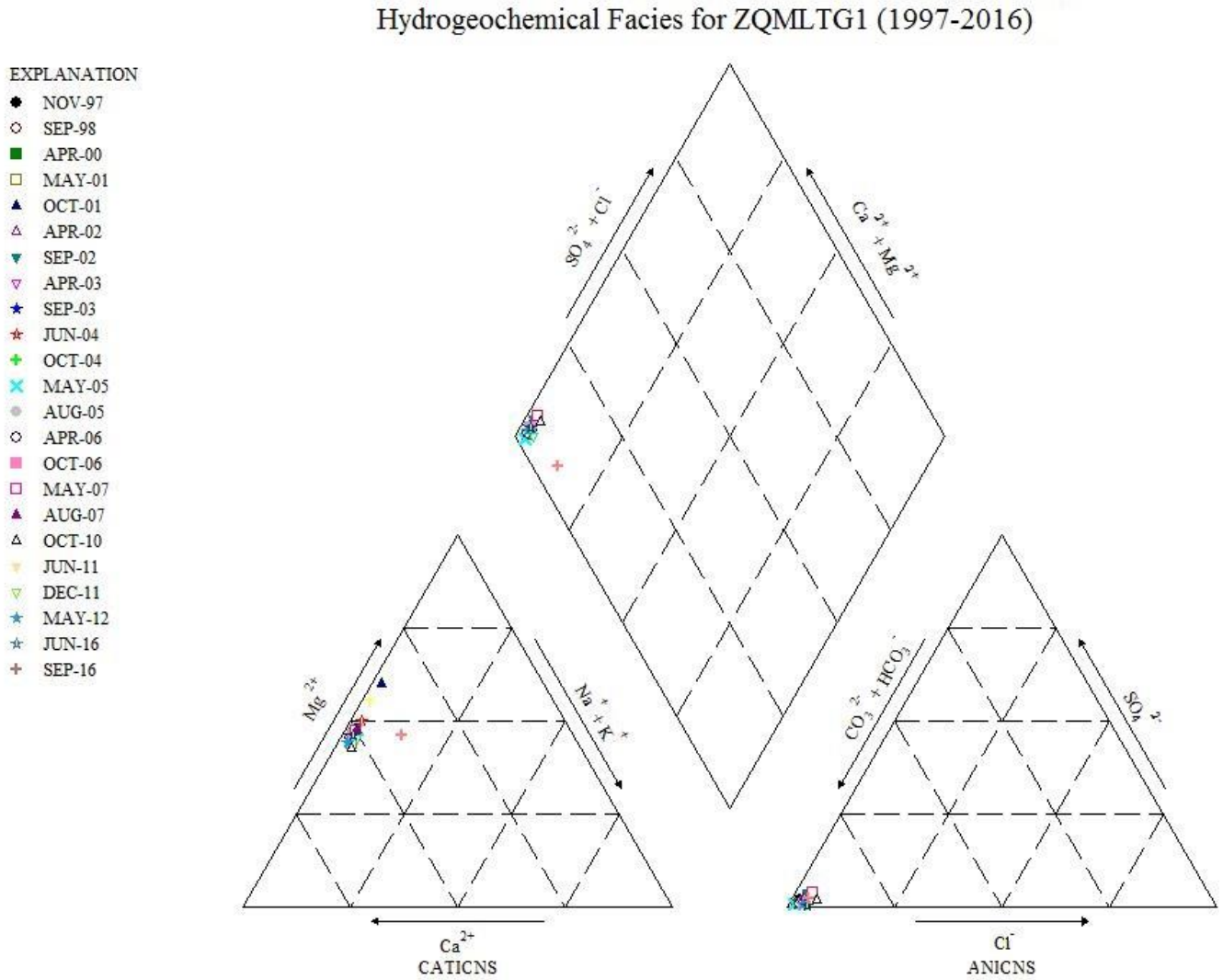


Figure 26: Piper diagram plot for major ions from 1997 to 2016 (ZQMLTG1)

From the piper diagram, data plotted in the same region despite varying climatic conditions. The only result that moved away from others was because of elevated Na (Sodium) in SEP-16, however the ion balance error was off by 0.8 %. Even with the elevated Na, all analysis still plot on the fresh water block of the piper diagram. Dolomite is the main aquifer geology that is rich in calcium and magnesium.

The main water facies is represented by Ca-Mg-HCO₃ type water. This is typical of dolomitic water. Clustering of groundwater was noted at this area from 1997 until 2016 as displayed in the piper diagram above.

Data from C3N0544 is presented together with the latest available data from ZQMLTG1 (September 2016) in order to determine if there are any similarities in terms of groundwater quality and facies.

Major ion data for C3N0544 plot in the same area as the historical data for ZQMLTG1 (Figure 26). However C3N0544 facies is classified as Ca-HCO₃ and ZQMLTG1 is classified as Ca-Mg-HCO₃ facies. The difference in facies is due to the chemical composition of the host rocks. C3N0544 is hosted by a calcium carbonate “limestone” (CaCO₃) which is free of magnesium. ZQMLTG1 is hosted by calcium magnesium bicarbonate “dolomite” [CaMg (CO₃)₂] which is rich in magnesium.

Composition of C3N0544 and ZQMLTG1

EXPLANATION

- C3N0544 (November 2017)
- ZQMLTG1 (September 2016)

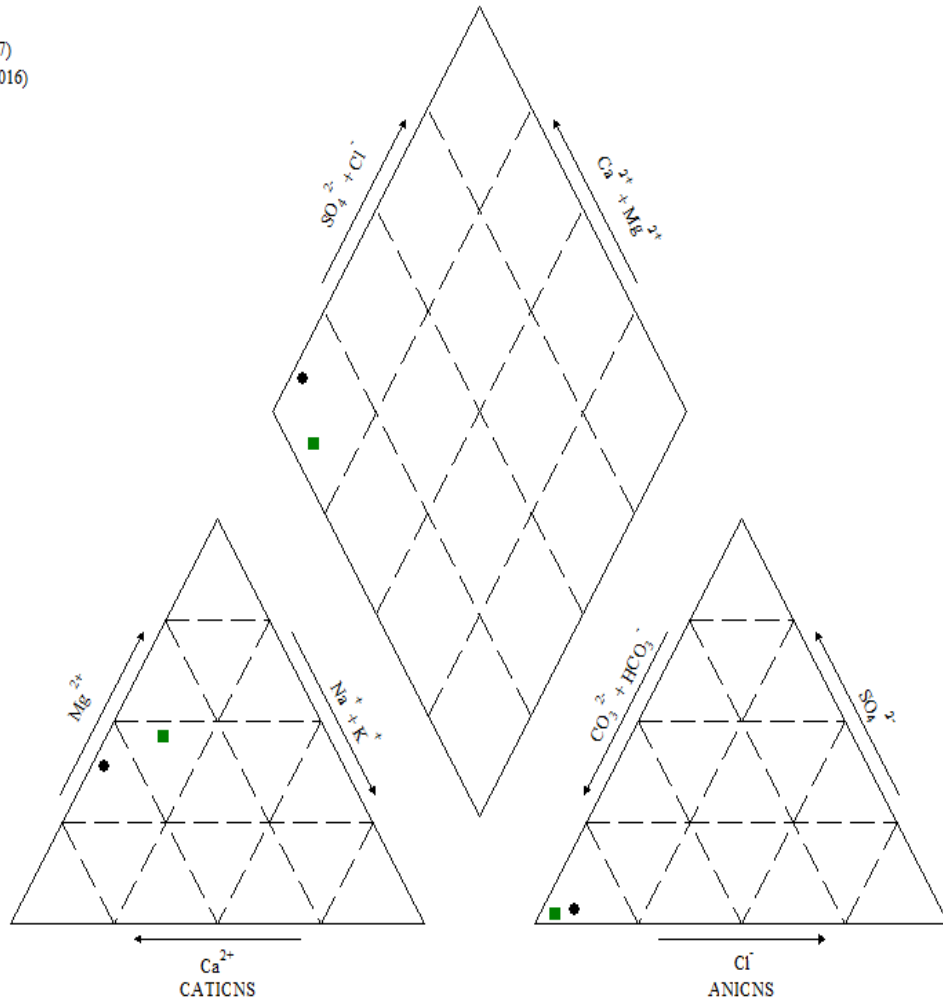


Figure 27: Piper diagram plot for C3N0544 and ZQMLTG1

5.4.2. Stable isotopes analysis

The isotopes analysis results are tabulated in Table 9 below. The isotopes plot against Pretoria LMWL is also presented in Figure 28 below.

Table 9: Stable isotopes results

Sample Name	Date of measurements	$\delta^2\text{H} \text{‰}$	$\pm^2\text{H}$ StDev	$\delta^{18}\text{O} \text{‰}$	$\pm^{18}\text{O}$ StDev
C3N0544	04/11/2017	-16.3	0.4	-2.92	0.0
C3N0036	04/11/2017	-24.3	2.0	-4.83	0.2
ZQMLTG1	04/11/2017	-27.0	0.3	-4.72	0.1
RAIN	04/11/2017	-13.4	0.4	-3.68	0.1

Rain sample plots above the LMWL and this could indicate condensation. Borehole C3N0544 plot below the LMWL, which indicates that evaporation took place before infiltration into the groundwater. The heavy isotope enrichment indicates the presence of evaporation before infiltration into the groundwater (summer samples). This can be attributed to seasonal effect.

Both C3N0036 and ZQMLTG1 are more depleted in ^{18}O and ^2H , which indicates mixing with deep circulating water (possibly karstic spring). Figure 28 also suggest that there was limited evaporation prior to infiltration in ZQMLTG1. C3N0036 plots along the LMWL and this indicate that no fractionation took place prior infiltration. This could also indicate locally limited shallow groundwater.

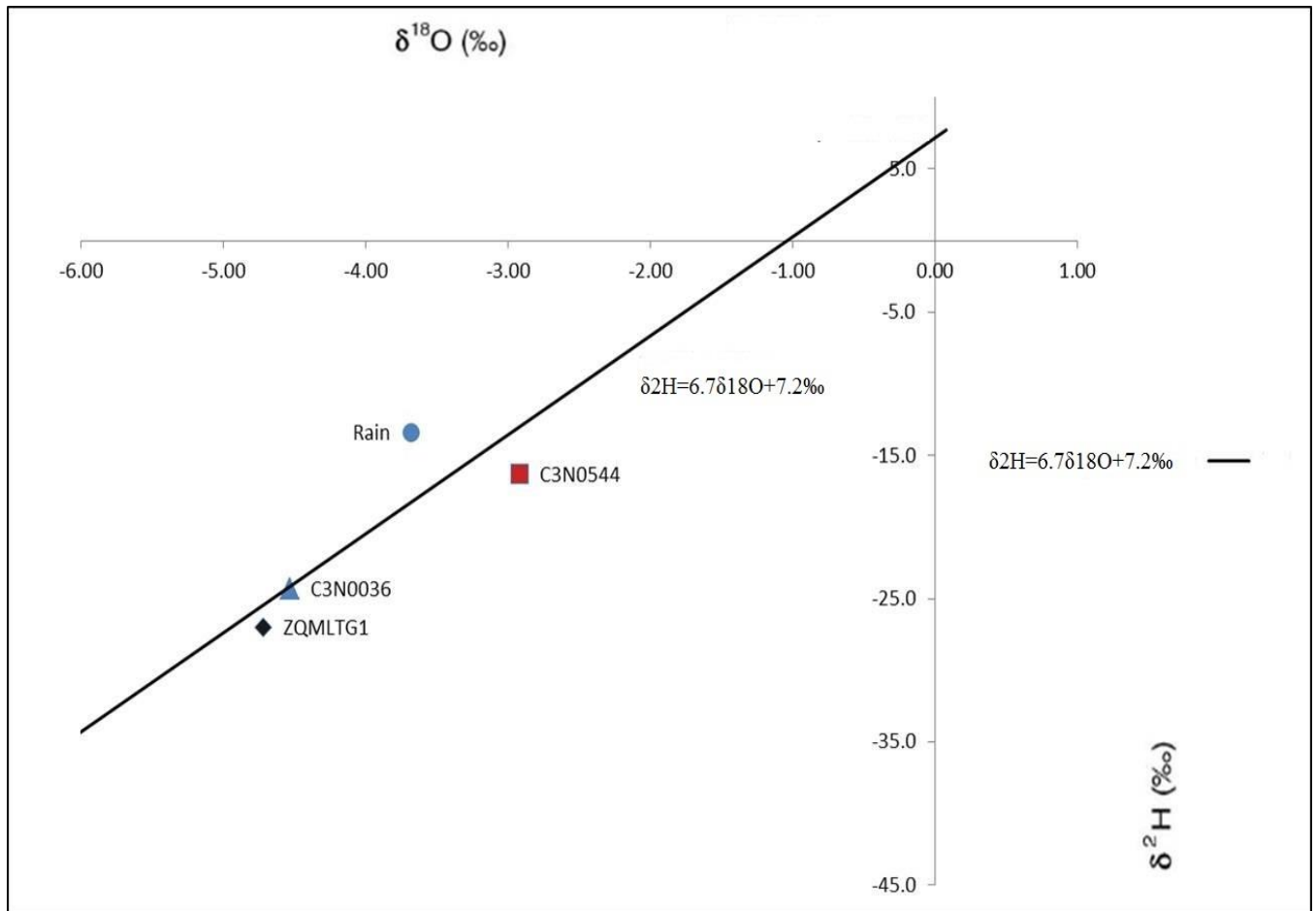


Figure 28: Stable isotope analysis plot on the Pretoria LMWL

5.5. Conceptual model

The conceptual model of the study area is presented in Figure 29 below. This conceptual model is based on the parameters collected in 2016/17 hydrological year. Groundwater levels presented in Table 3 were used to and a uniformly fractured aquifer was assumed in order to construct groundwater flow direction. Groundwater is flowing towards north eastern side of the study area where there is large groundwater abstraction for irrigation.

Mean annual precipitation was recorded as 720.8 mm/a and a maximum temperature of 32°C was assumed. Recharge in the study area was estimated as 20% (140.56 mm) of MAP. Total annual abstraction was estimated at 37 million m³/a. 8 million m³/a used for domestic water supply, municipality and industry are estimated to be abstracting 1.6 million m³/a and the main

abstraction is for irrigation estimated to be 28 million m³/a. All abstraction areas known are also indicated.

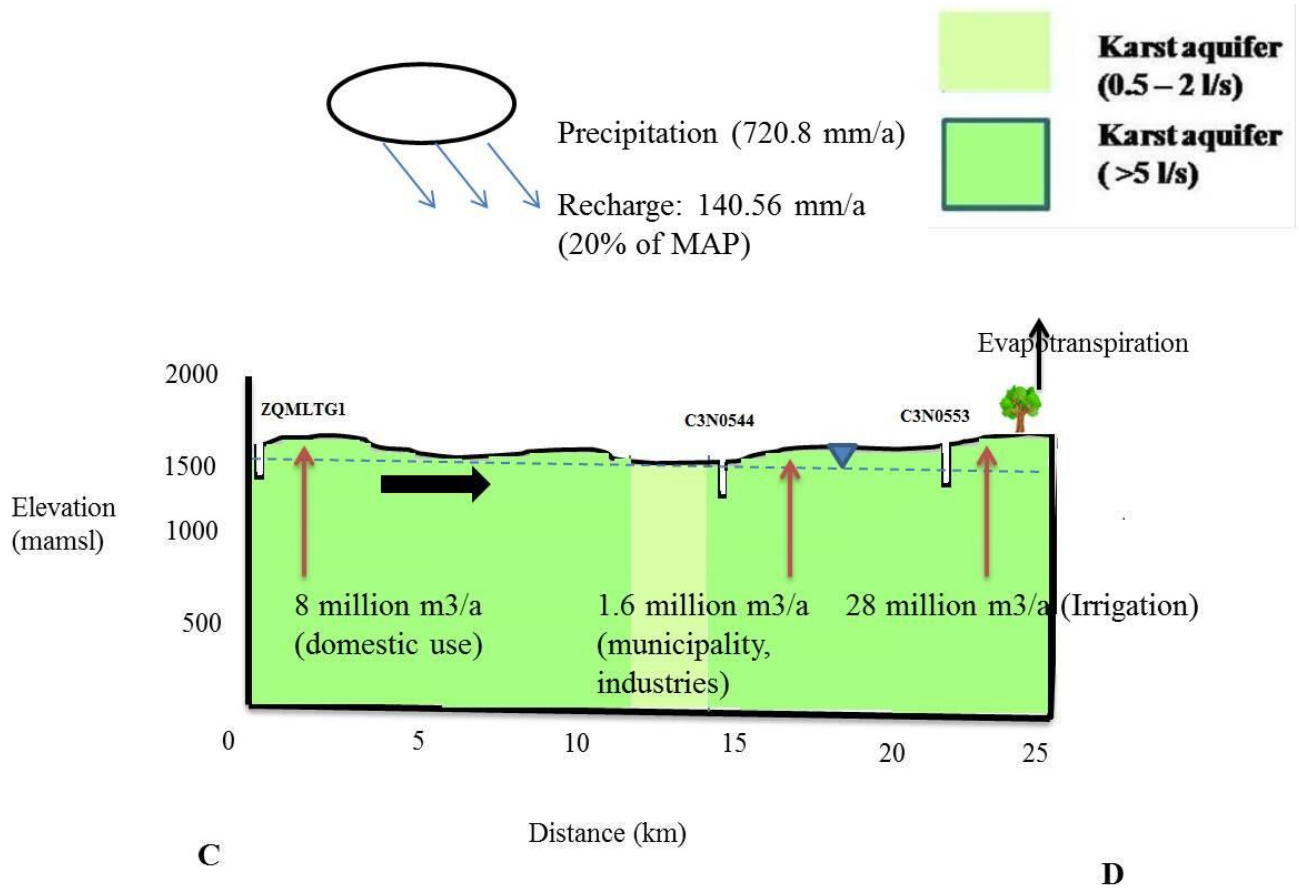


Figure 29: Conceptual hydrogeological model of the study area

Chapter 6: Conclusion

Various methodologies applied in this study managed to meet the main objectives of the study, which was to determine the extent of the impact of climatic variation on the dolomitic aquifer. All three groundwater level monitoring boreholes displayed a drop in the water table over the same period from 2013 to 2017. This can be attributed to climatic variation associated with the El Nino event in Southern Africa as well as abstraction in this quaternary catchment.

Actual sampling of chloride in rainfall and data from C3N0544 resulted in higher recharge estimation than linear relationship. The CMB recharge based on actual sampling estimated recharge for 2016/17 at 20 % (140.56 mm/a) of MAP. This correlates well with the sharp rise in groundwater table experienced in all three boreholes at the beginning of January 2017.

The declining groundwater table observed can be attributed to both climatic variation and abstraction. Groundwater table have been declining around the same period of climatic extremes (low rainfall, high temperature). Groundwater table continues to decline even during periods of high rainfall (moderately wet period) and high recharge and this is a possible indication that abstraction is also a key factor responsible for the declining groundwater table in this dolomitic aquifer. Soil moisture and high evapotranspiration are other possible sources related to the declining groundwater table.

The groundwater quality remained constant from 1997 until 2017. EC and pH were not affected by climatic variation and possible over-abstraction since 1997. Piper diagrams classified the groundwater as Ca-Mg-HCO₃ water which is typical fresh and shallow groundwater of Ca-Mg-HCO₃ facies. No evolution or mixing of groundwater in this aquifer in the last two decades.

Isotopes analysis revealed that evaporation took place before infiltration in one of the boreholes while the other two boreholes are more depleted. C3N0036 and ZQMLTG1 showed possible mixing with deep circulating karstic springs. Rainfall sample indicated that there was low humidity in the vapour during precipitation because the sample was taken summer.

This study concluded that climatic variation and/or abstraction are the main factors resulting in the declining of the groundwater table in this dolomitic aquifer of Lichtenburg.

Chapter 7: References

1. Abiye, T. 2016. Synthesis on groundwater recharge in Southern Africa: A supporting tool for groundwater users. *Groundwater for Sustainable Development* 2. 182-189.
2. Abiye, T., Masindi, K., Mengistu, H., & Demlie, M. 2018. Understanding the groundwater-level fluctuations for better management of groundwater resource: A case in the Johannesburg region. *Groundwater for Sustainable Development*. Vol.7, Pp.1-7.
3. Agricultural Research Council (ARC). 2016. Umlindi: The Watchman. Issue 2016-10. Institute for soil, climate and water, Pretoria, pp.4.
4. Agricultural Research Council (ARC). 2017. Umlindi: The Watchman. Issue 2017-07. Institute for soil, climate and water, Pretoria, pp.3-4.
5. Arora, V.K. 2002. The use of the aridity index to assess climate change effect on annual runoff. *J. Hydrol.*265, 164-177.
6. Barnard, H.C. 2000. An explanation of the 1:500 000 Hydrogeological map, Johannesburg 2526. Department of Water Affairs and Forestry (DWAf).
7. Beekman, H.E., Gieske, A., & Selaolo, E.T. 1996. Groundwater recharge studies in Botswana 1987-1996. *Botswana J. of Earth sci.* Vol. III, pp. 1-7.
8. Beekman, H.E., Selaolo, E.T., & De Vries, J.J. 1999. Groundwater recharge and resources assessment in the Botswana Kalahari. GRES II executive summary and technical report, pp. 48.
9. Beekman, H.E., & Xu, Y. 2003. Review of groundwater estimation in arid and semi-arid Southern Africa. In Xu, Y., & Beekman, H.E., (Eds). *Groundwater recharges estimation in Southern Africa*. UNESCO IHP series no.64, pp. 12.
10. Bouchaou, L., Tagma, T., Boutaleb, S., Hssaisoune, M., & El Morjani, Z.A. 2011. Climate change and its impacts on groundwater resources in Morocco: the case of the Souss-Massa basin. In: Treidel H, Martin-Bordes JL, Gurdak JJ, eds. *Climate Change Effects on Groundwater Resources: A Global Synthesis of Findings and Recommendations*. CRC Press (2011), 129-44.
11. Beukes, N.J. 1987. Facies relations, depositional environments and diagenesis in a major early Proterozoic stromatolitic carbonate platform to basinal sequence, Campbellrand Subgroup, Transvaal Supergroup, Southern Africa. *Journal of Sedimentary Geol.*, 54, 1-46.

12. Bogare Consultant. 2005. Welbedacht bulk water supply: Groundwater resource augmentation phase 1. Department of Water Affairs report 2.2(953), Pretoria.
13. Botha, L.J. 1993. Estimation of the Zeerust/Rietpoort groundwater potential. GH 3815 Report. Pretoria: Directorate of Geohydrology. P.18-25.
14. Braune, E., & Xu, Y. 2008. Groundwater management issues in Southern Africa- an IWRM perspective. Water SA 34 (6), 699-706.
15. Bredenkamp, D.B. 1964. Verslag van die hidrologiese opname in die Bo-Molopo ondergrondse waterbeheergebied. Unpub. Report GH 1283, Geohydrology division, Department of Environmental Affairs, Pretoria, pp.26.35.
16. Bredenkamp, D.B. 1987. Quantitative estimation of groundwater recharge in the Pretoria-Rietondale area. Technical report no. 3508, Department of Water Affairs, South Africa.
17. Bredenkamp, D.B. 1988. Ondersoek na beweerde invloed van die Bo-Molopo staatswaterskema op die olieendraaifontein van die Rietvallei/Weltevredesbesproeiingsraad. Department of Water Affairs and Forestry. GH Report 3602.
18. Bredenkamp, D.B. 1993. Hydrological evaluation of the West Rand dolomitic compartments: Zuurbekom, Gembokfontein East and Gembokfontein West. Department of water affairs and forestry, Technical Report GH 3866.
19. Bredenkamp, D.B. 1995. Dolomitic groundwater resources of the Republic of South Africa. Technical report 1 GH 3857, pp. 36-37, Directorate Geohydrology, DWAF.
20. Bredenkamp, D.B., &Zwarts, A. 1988. Ontginning van die Rietpoort grondwaterbron wat Zeerust van water voorsien. Technical Report GH 3603, Directorate Geohydrology, Department of Water Affairs and Forestry, Pretoria.
21. Bredenkamp, D.B., Botha, L.J., van Tonder, G.J., & Van Rensburg, H. 1995. Manual on qualitative estimation of groundwater recharge and aquifer storativity, based on practical hydro-logical methods. Water Research Commission. WRC report no. TT 73/95, Pretoria, South Africa, pp.407.
22. Bredenkamp, D.B. 1997. Dolomitic groundwater resources of the Republic of South Africa: Part 2. DWAF, GH Report 3857, pp. 18-21, Pretoria.

23. Bredenkamp, D.B., & Xu, Y. 2003. Perspective on recharge estimation in dolomitic aquifers in South Africa. In Xu, Y., & Beekman, H.E., (Eds). Groundwater recharges estimation in Southern Africa. UNESCO IHP series no.64, pp.67-69.
24. Bredenkamp, D.B., Vogel, J.C., Wiegmans, F.E., Xu, Y., & Van Rensburg, H. 2009. Use of natural isotopes and groundwater quality for improved estimation of recharge and flow in dolomitic aquifer. Water Research Commission. WRC report no. KV177/07, Pretoria, South Africa, pp. 43-44.
25. Bush, R.A. 1989. A geohydrological assessment of the Swartwater and Beauty areas, Northern western Transvaal. Directorate of geohydrology, Department of Water Affairs and Forestry, Pretoria, South Africa, Report no. GH 3577, pp.23.
26. Button, A. 1970. The stratigraphic history of the Malmani dolomite in the eastern and north eastern Transvaal. Johannesburg: Economic geology research unit. University of the Witwatersrand. P.1-26.
27. Calow, R.C., Macdonald, A.M., Nicol, A.L., & Robins, N.S. 2010. Groundwater security and drought in Africa: linking availability, access and demand. *Groundwater*, 48, 246-256.
28. Clark, I., & Fritz, P. 1997. Environmental isotopes in hydrogeology. Lewis publishers. New York, pg. 3228.
29. Clay, A.N. 1981. The geology of the Malmani Subgroup in the Carletonville area, Transvaal. Johannesburg: University of the Witwatersrand. Masters dissertation, unpub, pp. 55-61.
30. Coetzee, H.P.A. 1996. The stratigraphy and sedimentology of the Black Reef quartzite Formation, Transvaal sequence, in the area of Carletonville and the West-Rand goldfields, Potchefstroom: University for Christian higher education. Masters dissertation, unpub, pp. 9-71.
31. Cogho, V.E. 1982. Die ontginbare groundwater potensiaal van die grootfontein kompartement. Report No. GH 3242, Department of Water and Sanitation, Pretoria.
32. Council for Geosciences (CGS). 2015. South African geological hazards observation system ATLAS, pp.21.
33. Craig, H. 1961. Isotopic variation in meteoric water. *Science*, V.133, pp. 1702-1703.

34. Dennis, R & Dennis, I. 2012. Climate change vulnerability index for South African aquifers. In: Water SA Vol.38. No.3. International conference on groundwater special edition. 2012, pp. 417-426.
35. Department of Water Affairs & Forestry (DWAF). 2006. A guideline for assessment, planning and management of groundwater in South Africa. Volume 1: Conceptual introduction. Report no. 14/14/51, pp 9-18.
36. Department of Water Affairs & Forestry (DWAF). 2008. A guideline for assessment, planning and management of groundwater in South Africa. Volume 2, Final report no. 14/14/51, pp. 5-7.
37. Department of Water Affairs & Forestry (DWAF). 2006. Groundwater resource assessment: Dolomite aquifer. DWAF report no. P RSA C000/00/4466/06. Pp. 24-33.
38. Department of Water & Sanitations (DWS). 2016. Water scarcity and drought status report. NIWIS version 1, pp.2.
39. Enslin, J.P. 1970. Die groundwater potensiaal van Suid-Afrika. Convention: Water for the future, November 1970. Geological survey of South Africa, pp.169-180.
40. Eriksson, E., & Khunakasem, V. 1969. Chloride concentration in groundwater, recharge rate and rate of deposition of chloride in the Israel coastal plain. Journal of Hydrol. Vol. 7, pp.178-197.
41. Eriksson, P.G., Alterman, N.W., &Hartzler, F.J. 2006. The Transvaal Supergroup and its precursors. In: Johnson, M.R., Anhaeusser, C.R., & Thomas, R.J. (eds). The Geology of South Africa. GSSA/CGS, Johannesburg/ Pretoria, pp. 691/ pp. 237-260.
42. FAMINE EARLY WARNING SYSTEM NETWORK (FEWS.NET). 2014. Southern Africa special report: 2014/15 El Nino event, USAID, pp.1-2.
43. Felix, R., Olivier, L., Thierry, N., & Neil, H. 2015. The 2015-2016 El Nino event: expected impact on food security and main responses scenario in East and Southern Africa. EUR 27653 EN, JRC Science hub, pp.1-4.
44. Fleisher, J.N.E. 1981. Geohydrology of the dolomite aquifers of the Malmani Subgroup in the south-western Transvaal, RSA. Department of Water Affairs and Forestry, Technical Report GH 3169, pp. 27-31.
45. Forster, S. 1987. Fundamental concepts in aquifer vulnerability, pollution risk and protection strategy. International conference, 1987, Noordwyk Aan Zee, the Netherland

- vulnerability of soil and groundwater to pollutants. Netherland organization for applied scientific research, The Hague, 69-86.
46. Hem, J.D. 1985. Study and interpretation of the chemical characteristics of natural water. 3rd edition. USGS, pp.178-179.
 47. Holland, M. 2012. Evaluation of factors influencing transmissivity in fractured hard-rock aquifers of the Limpopo province. In: Water SA, Vol. 38, no. 3: pp.379-390. International conference on groundwater special edition 2012.
 48. Houston, J.F.T. 1988. Rainfall-runoff-recharge relationship in the basement rocks of Zimbabwe. In: Simmers, I (editor). Estimation of natural groundwater recharge. NATO ASI series C222, Reidel, Dordrecht, pp.349-366.
 49. Kumar, C.P. 2012. Climate change and its impact on groundwater resources. International journal of engineering and sciences. Vol.1, Issue 5, pp 46-49.
 50. Lerner, D.N., Issa, A., & Simmers, J. 1990. A guide to understanding and estimating natural recharge. International contribution to hydrogeology. Vol 8, Hannover, Verlag Heinz, pp.345.
 51. Loaiciga, H.A. 2003. Climate change and groundwater, Annals of the Association of American Geographers, Vol. 93 (1), pp. 30-41.
 52. Manatsa, D., Chingombe, W., Matsikwa, H., & Matarira, C.H. 2008. The superior influence of Darwin sea level pressure anomalies over ENSO as a simple drought predictor for Southern Africa. Theor. Appl. Climatol. 92, 1-14.
 53. Masih, I., Maskey, S, Mussa, F.E.F., & Trambauer, P. 2014. A review of droughts on the African continent: A geospatial and long-term perspective. Hydrol. Earth System. Sci., Vol. 18, pp. 3635-3679.
 54. Mckee, T.B., Doesken, N.J., & Kliest, J. 1993. The relationship of drought frequency and duration to time scale. In: Proceedings of the 8th conference of applied climatology. 17-22 January, Anaheim, CA. American meteorological society, Boston, MA, pp. 179-184.
 55. Meyer, R. 2005. Analysis of groundwater level time series and the relationship to rainfall and recharge. Water Research Commission, WRC Report no. 1323/1/05, Pretoria, South Africa, pp.17-20.
 56. Meyer, R. 2014. Hydrogeology of groundwater: Region 10, Karst Belt. Water Research Commission. WRC report no. TT 553/14, Pretoria, South Africa, pp.15.

57. Michaluk, E., & Moen, H.F.G. 1991. The geology of the Mafikeng area- Explanation sheet 2524 (1:250 000). Geol. Surv. S.Afri. p.45.
58. Obbes, A.M. 1995. The structure, stratigraphy and sedimentology of the Black Reef-Malmani-Rooihogte succession of the Transvaal Supergroup southwest of Pretoria. Pretoria: Council for Geosciences. P.1-89.
59. Obbes, A.M. 2001. The structure, stratigraphy and sedimentology of the Black-Reef-Malmani-Rooihogte succession of the Transvaal Supergroup southwest of Pretoria. CGS Bulletin 127. CGS, Pretoria. P.89.
60. Panda, D.K., Mishra, A., & Kumar, A. 2012. Quantification of trends in groundwater levels of Gujarat in Western India. Hydrological Sciences Journal, 57:7, 1325-1336.
61. Pyburn, M.R. 2015. The hydrogeological relationship between recharge, abstraction and spring flow in the Zeerust dolomite aquifer. Masters dissertation, North West University, unpub, pp. 84-86.
62. Polivka, J. 1987. An investigation of the Ventersdorp and Grootpan compartment in the Western Transvaal. Technical report GH 3524, Department of Water Affairs and Forestry, Pretoria, pp.19-20.
63. Richard, Y., Fauchereau, N., Pocard, I., Rouault, M., & Trzaska, S. 2001. 20th century droughts in Southern Africa: Spatial and temporal variability, teleconnections with oceanic and atmospheric conditions. Int.J.Climatol, 21, 873-885.
64. Rouault, M., & Richard, Y. 2005. Intensity and spatial extent of droughts in Southern Africa. Geophys. Res. Lett., 32, L15702.
65. Simmers, I. 1988. Estimation of natural groundwater recharge. NATO ASI series C. Vol.222, pp.510. Proc. Of the NATO advanced research workshop, Antalya, Turkey.
66. Singh, R.D., & Kumar, C.P. 2010. Impact of climate change on groundwater resources. Natural institute of hydrology, Roorkee- 247667 (Uttarakhand), 1-8.
67. South African Council for Stratigraphy (SACS). 1980. Stratigraphy of South Africa. Part 1. Lithostratigraphy of the Republic of South Africa, Namibia and the Republics of Bophuthatswana, Transkei and Venda: Handbook of the Geological survey of South Africa, 8, 690 pp.
68. Stagl, J., Mayr, E., Hattermann, F.F., & Huang, S. 2014. Effects of climate change on the hydrological cycle in Central and Eastern Europe. In: Rannow, S., & Neubert, M. (eds)

Managing protected areas in Central and Eastern Europe under climate change. *Advances in global change research*, vol 58, pp.31-43. Springer, Dordrecht.

69. Sun, H. 2005. Estimating shallow groundwater recharge in the headwaters of the Liverpool plains using SWAT. Vol.19, issue 3, pp.795-807. Western Sydney University.
70. United Nations Development Programme (UNDP). 2017. UNDP's response to El Nino and La Nina. New York, USA, pp.1-7.
71. Van Tonder, G.H., Janse Van Rensburg, H., Botha, J.F., & Bredenkamp, D.B. 1986. Die modellering van grondwatervlakke in die Grootfontein compartment in Wes-Transvaal. *Water SA* 12 (3), pp 151-160.

